Electrostatic Forces between Surfaces in Liquids

14.1 The Charging of Surfaces in Liquids: the Electric "Double-Layer"

Situations in which van der Waals forces alone determine the total interaction are restricted to a few simple systems—for example, to interactions in vacuum or to nonpolar wetting films on surfaces, both of which were discussed in Chapter 13. In more complex, and more interesting, systems long-range electrostatic forces are also involved, and the interplay between these two interactions has many important consequences.

As mentioned earlier the van der Waals force between similar particles in a medium is always attractive, so that if only van der Waals forces were operating, we might expect all dissolved particles to stick together (coagulate) immediately and precipitate out of solution as a mass of solid material. Our own bodies would be subject to the same fate if we remember that we are composed of 55–75% water. Fortunately this does not happen, because particles suspended in water or any liquid of high dielectric constant are usually charged and can be prevented from coalescing by repulsive electrostatic forces. Other repulsive forces that can prevent coalescence are solvation and steric forces, described in Chapters 15 and 16. In this chapter we shall concentrate on the electrostatic forces.

The charging of a surface in a liquid can come about in three ways:

- 1. By the ionization or dissociation of surface groups (e.g., the dissociation of protons from surface carboxylic groups ($-COOH \rightarrow -COO^- + H^+$), which leaves behind a negatively charged surface)
- **2.** By the adsorption or binding of ions from solution onto a previously uncharged surface—for example, the adsorption of $-OH^-$ groups to the water-air or water-hydrocarbon interfaces that charges them negatively, or the binding of Ca^{2+} onto the zwitterionic headgroups of lipid bilayer surfaces that charges them positively. The adsorption of ions from solution can, of course, also occur onto oppositely charged surface sites—for example, the adsorption of cationic Ca^{2+} to anionic $-COO^-$ sites vacated by H^+ or Na^+ . Such surfaces are known as *ion exchangeable* surfaces. Ion exchange can take a surprisingly long time.
- **3.** The above examples apply to isolated surfaces exposed to a liquid medium (usually water). A different type of *charge exchange* mechanism occurs between two dissimilar

surfaces very close together where, as previously mentioned in Section 3.5, charges usually protons or electrons—hop across from one surface to the other. This gives rise to an electrostatic attraction between the now oppositely charged surfaces. Such "acid-base" type interactions are important for understanding short-range adhesion forces and are discussed in Chapter 17.

Whatever the *charging mechanism* (also referred to as *charge regulation*), the final surface charge of *co-ions* is balanced by an equal but oppositely charged region of *coun*terions. Some of the counterions are bound, usually transiently, to the surface within the socalled Stern or Helmholtz layer, while others form an atmosphere of ions in rapid thermal motion close to the surface, known as the diffuse *electric double-layer*¹ (Figure 14.1). The difference between a "bound" ion and a "free" ion in the diffuse double-layer is analogous to the difference between a water molecule in the sea and in the atmosphere. However, because the distances involved in the latter case are of atomic dimensions, the distinction can sometimes become blurred.

Two similarly charged surfaces usually repel each other electrostatically in solution, though under certain conditions they may attract at small separations. Zwitterionic surfaces—that is, those characterized by surface dipoles but no net charge also interact electrostatically with each other, though here we shall find that the force is usually attractive.

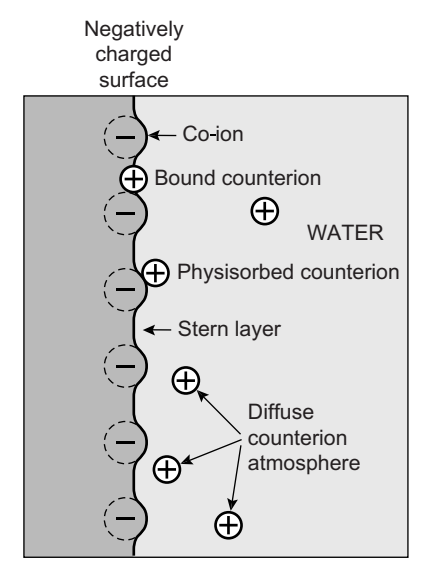


FIGURE 14.1 lons bound to a surface are not rigidly bound but can exchange with other ions in solution; their lifetime on a surface can be as short as 10^{-9} s (1 ns) or as long as many hours.

¹Originally, the layers of co-ions and counterions were thought to behave like a capacitor whose two rigid plates carry equal but opposite charges (see Section 3.3). Hence the term "double-layer" [of charge]. Indeed, capacitors are excellent models for double-layers as far as their electrical properties are concerned.

Charged Surfaces in Water: No Added 14.2 Electrolyte—"Counterions Only"

In the following sections we shall consider the counterion distribution and force between two similarly charged planar surfaces in a pure liquid such as water, where (apart from the H₃O⁺ and OH⁻ ions from dissociated water) the only ions in the solution are those that have come off the surfaces. Such systems are sometimes referred to as "counterions only" systems, and they occur when, for example, colloidal particles, clay sheets, surfactant micelles or bilayers whose surfaces contain ionizable groups interact in pure water, and also when thick films of water build up (condense) on an ionizable surface such as glass. But first we must consider some fundamental equations that describe the counterion distribution between two charged surfaces in solution.

14.3 The Poisson-Boltzmann (PB) Equation

For the case when only counterions are present in solution, the chemical potential of any ion may be written as (cf. Sections 2.3 and 2.4):

$$\mu = ze\psi + kT\log\rho,\tag{14.1}$$

where ψ is the electrostatic potential ($E = -d\psi/dx$ is the electric field), and ρ the number density of ions of valency z at any point x between two surfaces (Figure 14.2). Since only differences in potential are ever physically meaningful, we may set $\psi_0 = 0$ at the midplane (x = 0), where also $\rho = \rho_0$ and $(d\psi/dx)_0 = 0$ by symmetry.

From the equilibrium requirement that the chemical potential be the same throughout (i.e., for all values of x), Eq. (14.1) gives us the expected Boltzmann distribution of counterions at any point x (the Nernst equation):

$$\rho = \rho_0 e^{-ze\psi/kT}. \tag{14.2}$$

One further important fundamental equation is required. This is the well-known Poisson equation for the net excess charge density at x:

$$ze\rho = -\varepsilon_0 \varepsilon (d^2 \psi / dx^2) \tag{14.3}$$

which when combined with the Boltzmann distribution, Eq. (14.2), gives the Poisson-Boltzmann (PB) equation:

$$d^{2}\psi/dx^{2} = -ze\rho/\varepsilon_{0}\varepsilon = -(ze\rho_{0}/\varepsilon_{0}\varepsilon)e^{-ze\psi/kT}.$$
 (14.4)

When solved, the PB equation gives the potential ψ , electric field $E = -\partial \psi/\partial x$, and counterion density ρ , at any point x in the gap between the two surfaces. Let us first determine these values at the surfaces themselves. These quantities are often referred to as the *contact values*: ψ_s , E_s , ρ_s , and so on.

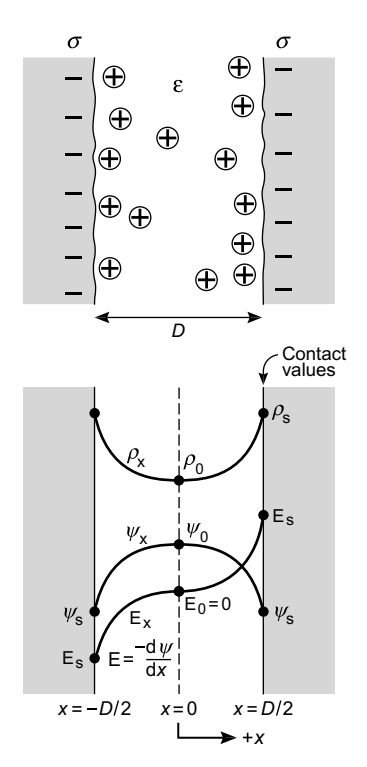


FIGURE 14.2 Two negatively charged surfaces of surface charge density σ separated a distance D in water. The only ions in the space between them are the counterions that have dissociated from the surfaces. The counterion density profile $\rho_{\rm x}$ and electrostatic potential $\psi_{\rm x}$ are shown schematically in the lower part of the figure. The "contact" values are $\rho_{\rm s}$, $\psi_{\rm s}$ and $E_{\rm S} = -({\rm d}\psi/{\rm d}x)_{\rm S}$.

14.4 Surface Charge, Electric Field, and Counterion Concentration at a Surface: "Contact" Values

The PB equation is a nonlinear second-order differential equation, and to solve for ψ we need two *boundary conditions*, which determine the two integration constants. The first boundary condition follows from the symmetry requirement that the field must vanish at the midplane—that is, that $E_0 = -(\mathrm{d}\psi/\mathrm{d}x)_0 = 0$. The second boundary condition follows from the requirement of overall *electroneutrality*—that is, that the total charge of the counterions in the gap must be equal (and opposite) to the charge on the surfaces. If σ is the surface charge density on each surface (in C m⁻²) and D is the distance between the surfaces (see Figure 14.2), then the condition of electroneutrality implies that

$$\sigma = -\int_0^{D/2} z e \rho \mathrm{d}x = + \varepsilon_0 \varepsilon \int_0^{D/2} (\mathrm{d}^2 \psi / \mathrm{d}x^2)^2 \mathrm{d}x = -\varepsilon_0 \varepsilon (\mathrm{d}\psi / \mathrm{d}x)_{D/2} = -\varepsilon_0 \varepsilon (\mathrm{d}\psi / \mathrm{d}x)_\mathrm{S} = -\varepsilon_0 \varepsilon E_\mathrm{S},$$

that is,

$$E_{S} = -\sigma/\varepsilon_{0}\varepsilon, \tag{14.5}$$

which is essentially Gauss' Law (cf. Section 3.4). Equation (14.5) gives an important general boundary condition relating the surface charge density σ to the electric field $E_{\rm s}$ at each surface (at $x=\pm D/2$), which we may note is independent of the gap width D.

Worked Example 14.1

Question: Is the electric field near a charged surface in water sufficiently intense to immobilize the water molecules adjacent to it?

Answer: Assuming a high-charge density of $\sigma = -0.3 \,\mathrm{C}\,\mathrm{m}^{-2}$ (which is one charge per $0.5 \,\mathrm{nm}^2$ typical of a fully ionized surface), the electric field at the surface. Eq. (14.5), is $E_s = -\sigma/\varepsilon_0 \varepsilon$ $-0.3/80(8.85 \times 10^{-12}) = -4.2 \times 10^8 \text{ V m}^{-1}$. We may compare this to the field just outside a monovalent ion in water. Using Eq. (3.1), the field at r = 0.25 nm from the center of an ion is $E_{\rm r} = e/4\pi\varepsilon_0\varepsilon r^2 = 2.9\times10^8~{\rm V~m^{-1}}$. Since this is comparable to the field at the charged surface, and since the fields of monovalent ions are usually not strong enough to immobilize water molecules around them (cf. Chapters 3-5), it is unlikely that water molecules will become significantly oriented, immobilized or "bound" to any but the most highly charged surfaces. However, other interactions with the surface, such as H-bonding, may lead to significant effects on the local water structure.

Turning now to the *ionic concentrations*, there exists an important general relation between the concentrations of counterions at either surface and at the midplane. Differentiating Eq. (14.2) and then using Eq. (14.4) we obtain

$$\frac{\mathrm{d}\rho}{\mathrm{d}x} = -\frac{ze\rho_0}{kT}e^{-ze\psi/kT}\left(\frac{\mathrm{d}\psi}{\mathrm{d}x}\right) = \frac{\varepsilon_0\varepsilon}{kT}\left(\frac{\mathrm{d}\psi}{\mathrm{d}x}\right)\left(\frac{\mathrm{d}^2\psi}{\mathrm{d}x^2}\right) = \frac{\varepsilon_0\varepsilon}{2kT}\frac{\mathrm{d}}{\mathrm{d}x}\left(\frac{\mathrm{d}\psi}{\mathrm{d}x}\right)^2,\tag{14.6}$$

hence

$$\rho_x - \rho_0 = \int_0^x \mathrm{d}\rho = \frac{\varepsilon_0 \varepsilon}{2kT} \int_0^x \mathrm{d}\left(\frac{\mathrm{d}\psi}{\mathrm{d}x}\right)^2 = +\frac{\varepsilon_0 \varepsilon}{2kT} \left(\frac{\mathrm{d}\psi}{\mathrm{d}x}\right)_x^2$$

so that

$$\rho_x = \rho_0 + \frac{\varepsilon_0 \varepsilon}{2kT} \left(\frac{\mathrm{d}\psi}{\mathrm{d}x}\right)_x^2,\tag{14.7}$$

which gives ρ at any point x in terms of ρ_0 at the midplane and $(d\psi/dx)^2$ at x. In particular at the surface, x = D/2, we obtain using Eq. (14.5) the contact value of ρ

$$\rho_s = \rho_0 + \sigma^2 / 2\varepsilon_0 \varepsilon kT. \tag{14.8}$$

This important result shows that the concentration of counterions at the surface depends only on the surface charge density σ and the counterion concentration at the midplane. It shows that ρ_s never falls below $\sigma^2/2\varepsilon_0\varepsilon kT$ even for isolated surfaces—that is, for two surfaces far apart when $\rho_0 \to 0$. For example, for an isolated surface in water of charge density $\sigma = -0.2 \text{ C m}^{-2}$ (one charge per 0.8 nm²) at 293 K

$$\rho_{\rm s} = \sigma^2/2\varepsilon_0\varepsilon kT = (0.2)^2/(2\times80\times8.85\times10^{-12}\times4.04\times10^{-21}) = 7.0\times10^{27}~{\rm m}^{-3},$$

which is about 12 M. If these surface counterions are considered to occupy a layer of thickness ~0.2 nm, the above value for ρ_s corresponds to a surface counterion density of $(7 \times 10^{27})(0.2 \times 10^{-9}) = 1.4 \times 10^{18}$ ions/m² or one charge per 0.7 nm², which is about the same as the surface charge density σ . This is an interesting result, for it shows that regardless of the counterion distribution profile ρ_r away from a surface (Section 14.5), most of the counterions that effectively balance the surface charge are located in the first few ångstroms from the surface (Jönsson et al., 1980)—that is, right up against the surface, hence the term double-layer. However, for lower surface charge densities, since $\rho_s \propto \sigma^2$, the layer of counterions extends well beyond the surface and becomes much more diffuse, hence the term diffuse double-layer.

14.5 Counterion Concentration Profile Away from a Surface

The above equations are quite general and are the starting point of all theoretical computations of the ionic distributions near planar charged surfaces, even when the solution contains added electrolyte (Section 14.10 onwards). To proceed further for the specific case of counterions only (see Figure 14.2) we must now solve the Poisson-Boltzmann equation, Eq. (14.4), which can be satisfied by²

$$\psi = (kT/ze)\log(\cos^2 Kx) \tag{14.9}$$

or

$$e^{-ze\psi/kT} = 1/\cos^2 Kx, \tag{14.10}$$

where *K* is a constant given by

$$K^2 = (ze)^2 \rho_0 / 2\varepsilon_0 \varepsilon kT. \tag{14.11}$$

With this form for the potential we see that $\psi = 0$ and $d\psi/dx = 0$ at x = 0 for all K, as required. To solve for K we differentiate Eq. (14.9) and then use Eq. (14.5) to obtain for the electric fields

at any point
$$x: E_x = -d\psi/dx = +(2kTK/ze)\tan Kx$$
, (14.12a)

at the surfaces :
$$E_s = -(d\psi/dx)_s = +(2kTK/ze)\tan(KD/2) = -\sigma/\varepsilon_0\varepsilon$$
. (14.12b)

²There are other mathematical solutions to this equation, but Eq. (14.9) is the only one that is physically realistic—that is, satisfying all the boundary conditions, as demonstrated further in the following.

The counterion distribution profile

$$\rho_x = \rho_0 e^{-ze\psi/kT} = \rho_0/\cos^2 Kx \tag{14.13}$$

is therefore known once K is determined from Eq. (14.12) in terms of σ and D.

Worked Example 14.2

Question: Two charged surfaces with $\sigma = 0.2$ C m⁻² are 2 nm apart (D = 2 nm). Calculate the field, potential and counterion density at each surface, at 0.2 nm from each surface and at the midplane, assuming monovalent counterions.

Answer: From Eq. (14.12) we find that for z=-1, $K=1.3361\times 10^9~{\rm m}^{-1}$ at 293 K. From Eq. (14.11) this means that $\rho_0 = 0.40 \times 10^{27} \, \mathrm{m}^{-3}$, so that at the surface $\rho_s = \rho_0/\cos^2(KD/2) = 7.4 \times 10^{12} \, \mathrm{m}^{-3}$ 10^{27} m⁻³. The same result is also immediately obtainable from Eq. (14.8), since, as we have previously established, $\sigma^2/2\varepsilon_0 \epsilon kT = 7.0 \times 10^{27} \text{ m}^{-3}$. Thus, the counterion concentration at each surface ρ_s is about 18.5 times greater than at the midplane ρ_0 , which is only 1 nm away. Putting $K = 1.3661 \times 10^9 \,\mathrm{m}^{-1}$, $kT = 4.045 \times 10^{-21} \,\mathrm{J}$, $\sigma = 0.2 \,\mathrm{Cm}^{-2}$, $\varepsilon = 80$, $ze = 1.602 \times 10^{-19} \,\mathrm{C}$, and $D = 0.000 \,\mathrm{Cm}^{-2}$ 2×10^{-9} m into Eqs. (14.9), (14.12), and (14.13), we obtain:

	ψ (mV)	E (V m ⁻¹)	$ ho~(\mathrm{m}^{-3})$
At $x = 1$ nm ("contact value" at surface)	74	2.8×10^8	$7.4 \times 10^{27} (12 \text{ M})$
At $x = 0.8$ nm (0.2 nm from surface)	37	1.2×10^{8}	$1.7 \times 10^{27} \text{ (3 M)}$
At $x = 0$ ("midplane" value 1 nm from surface)	0	0	$0.4 \times 10^{27} (0.7 \text{ M})$

Note the unphysically steep decrease in the ion density ρ near the surface over a distance of only 0.2 nm (2 Å).

Figure 14.3 shows how the counterion concentration varies with distance for the case of $\sigma = 0.224$ C m⁻², D = 2.1 nm, as calculated on the basis of (1) the Poisson-Boltzmann

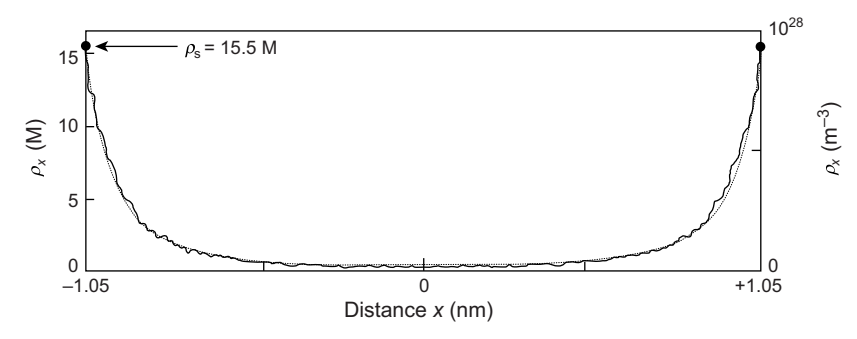


FIGURE 14.3 Monovalent counterion concentration profile between two charged surfaces ($\sigma = 0.224$ C m⁻², corresponding to one electronic charge per 0.714 nm²) a distance 2.1 nm apart in water. The smooth curve is obtained from the Poisson-Boltzmann equation; the other is from a Monte Carlo simulation by Jönsson et al., (1980).

equation as in the above example, and (2) a Monte Carlo simulation of the same system. The agreement is quite good though the Monte Carlo result gives a slightly higher counterion concentration very near the surfaces compensated by a lower concentration in the central region between the two surfaces.

14.6 Origin of the Ionic Distribution, Electric Field, Surface Potential, and Pressure

Before we proceed to calculate the force or pressure between two surfaces, it is instructive to discuss, in qualitative terms, how the counterion distribution, potential, field, and pressure between two surfaces arise. The first thing to notice is that if there were no ions between two similarly charged surfaces, there would be no electric field in the gap between them. This is because the field emanating from a planar charged surface, $E = -\sigma/2\varepsilon_0\varepsilon$, is uniform away from the surface (Section 3.3). The two opposing fields emanating from the two plane parallel surfaces therefore cancel out to zero between the two surfaces or plates (although they add up outside the two plates). Thus, when the counterions are introduced into the intervening region they do not experience an attractive electrostatic force toward each surface. The reason why the counterions build up at each surface is simply because of their mutual repulsion and is similar to the accumulation of mobile charges on the surface of any charged conducting material such as a metal. The repulsive electrostatic interaction between the counterions and their entropy of mixing alone determine their concentration profile ρ_x , the potential profile ψ_x and the field E_x between the surfaces (Jönsson et al., 1980), and we may further note that in all the theoretical derivations so far the only way the surface charge density σ enters into the picture is through Eq. (14.5), which is simply a statement about the total number of counterions in the gap.

Further, if the centers of the surface coions were not at the physical solid-liquid interface (at $x=\pm\frac{1}{2}D$) but at some small distance δ within the surface (Figure 14.4), the ionic distribution ρ_x , potential ψ_x , field E_x , and the pressure in the medium between $+\frac{1}{2}D$ and $-\frac{1}{2}D$ would not change. But the potential would be different if it were measured at $x=\pm(\frac{1}{2}D-\delta)$. This is the origin of the so-called *Stern* and *Helmholtz layers* (Stern, 1924; Verwey and Overbeek, 1948; Hiemenz, 1997) that separate the charged plane from the *Outer Helmholtz Plane* (OHP) from which the ionic atmosphere begins to obey the Poisson-Boltzmann equation. The combined thickness of the Stern and Helmholtz layers δ is of the order of a few ångstroms and reflects the finite size of the charged surface groups (coions) and transiently bound counterions, as illustrated in Figures 14.1 and 14.4. Clearly, within this region, whose thickness is determined by the finite (hard core) sizes of the ions, the PB equation cannot hold. If the dielectric constant of the Stern-Helmholtz layer is assumed to be uniform and equal to ε_{δ} it can be modeled as a capacitor (see Section 3.3) whence the additional drop in potential across this layer is given by

$$\psi_{\delta} = \sigma \delta / \varepsilon_0 \varepsilon_{\delta}. \tag{14.14}$$

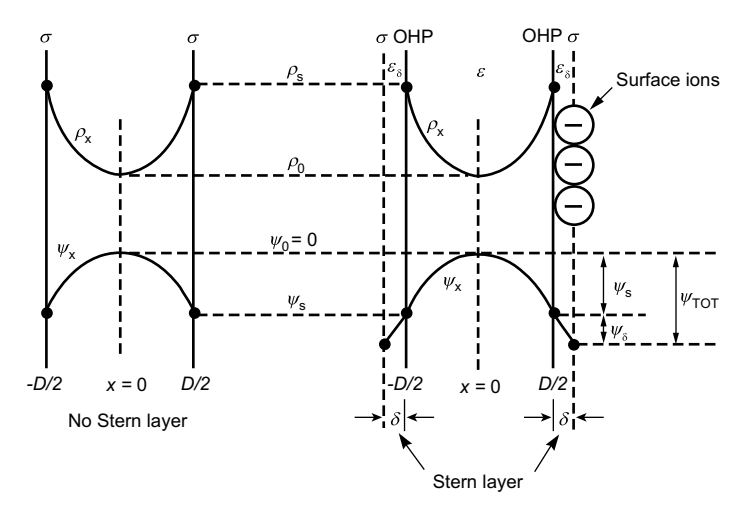


FIGURE 14.4 Stern layers of thickness \hat{b} at each surface dividing the planes of fixed charge density σ from the boundary of the aqueous solution—the OHP. There is an additional linear drop in potential across the Stern layer given by Eq. (14.14) so that the total potential drop is $\psi_{TOT} = \psi_{\delta} + \psi_{s}$. However, the counterion density and electrostatic potential within the agueous region between the two OHPs at x = D/2 and x = -D/2, and the pressure between the two surfaces, are independent of δ .

For example, if $\delta = 0.2$ nm, $\sigma = 0.2$ C m⁻², and $\varepsilon_{\delta} = 40$, we obtain $\psi_{\delta} = 130$ mV, which is actually higher than the potential drop across the diffuse double-layer, calculated in the previous worked example.

We now turn to the origin of the force or pressure between the two surfaces. Contrary to intuition, the origin of the repulsive force between two similarly charged surfaces in a solvent containing counterions and/or added electrolyte ions is entropic (osmotic), not electrostatic. Indeed, the electrostatic contribution to the net force is actually attractive. Consider an isolated surface, initially uncharged, placed in water. When the surface groups dissociate the counterions leave the surface against the attractive Coulombic force pulling them back. What maintains the diffuse double-layer is the repulsive osmotic pressure between the counterions which forces them away from the surface and from each other so as to increase their configurational entropy. On bringing two such surfaces together one is therefore forcing the counterions back onto the surfaces against their preferred equilibrium state—that is, against their osmotic repulsion but favored by the electrostatic interaction. The former dominates and the net force is repulsive.

On the other hand, to understand why the purely electrostatic part of the interaction is attractive recall that it involves an equal number of positive (counterion) and negative (surface) charges—that is, the system is overall electrically neutral. The net Coulombic interaction between a system of charges that are overall neutral always favors their association, as we saw in the case of ionic crystals in Chapter 3 and dipoles in Chapter 4.

There are situations where the electrostatic attraction does dominate over the entropic repulsion, giving rise to an overall attraction even between two equally charged surfaces or particles in solution. These cases are discussed in later Sections.

The Pressure between Two Charged Surfaces 14.7 in Water: the Contact Value Theorem

We may derive an expression for the pressure of counterions in a confined space in the same way as the pressure of a van der Waals gas in a confined volume was derived in Section 2.5. Using Eq. (2.20), the repulsive pressure P of the counterions at any position x from the center (see Figure 14.4) is given by $(\partial P/\partial x')_{x,T} = \rho(\partial \mu/\partial x')_{x,T}$, where the chemical potential μ is given by Eq. (14.1). The change in pressure at x on bringing two plates together from infinity ($x' = \infty$, where P = 0) to a separation x' = D at constant temperature is therefore

$$P_{x}(D) - P_{x}(\infty) = P_{x}(D) = + \int_{\infty}^{D} \left[ze\rho(d\psi/dx')dx' + kT(d\rho/dx')dx' \right]$$
$$= - \int_{x'=D}^{x'=\infty} \left[ze\rho(d\psi/dx')_{x}dx' + kTd\rho_{x} \right]. \tag{14.15}$$

Note that in Eq. (14.15), the values are computed at a *fixed* point x within the ionic solution, which is not the same as the *variable* separation x' between the two surfaces. Replacing zep by the Poisson equation, Eq. (14.3), and using the relation

$$\frac{\mathrm{d}}{\mathrm{d}x} \left(\frac{\mathrm{d}\psi}{\mathrm{d}x} \right)^2 = 2 \left(\frac{\mathrm{d}\psi}{\mathrm{d}x} \right) \left(\frac{\mathrm{d}^2\psi}{\mathrm{d}x^2} \right)$$

Eq. (14.15) becomes

$$P_{x}(D) - P_{x}(\infty) = \left[-\frac{1}{2} \varepsilon_{0} \varepsilon \left(\frac{\mathrm{d}\psi}{\mathrm{d}x} \right)_{x(D)}^{2} + kT \rho_{x(D)} \right] - \left[-\frac{1}{2} \varepsilon_{0} \varepsilon \left(\frac{\mathrm{d}\psi}{\mathrm{d}x} \right)_{x(\infty)}^{2} + kT \rho_{x(\infty)} \right], \tag{14.16}$$

where the subscripts x mean that the values are calculated at x when the surfaces are at a distance *D* or ∞ apart. In the present case, since there are no electrolyte ions in the bulk solution, $\rho_0(\infty) = 0$, so that by Eq. 14.7, we have $P_x(\infty) = 0$, as expected.

The above important equation gives the pressure P at any point x between the two surfaces, and we may notice that it is split into two contributions. The first, being a square, is always negative—that is, attractive (except at the midplane, x = 0, where it is zero). This is the electrostatic field energy contribution, discussed qualitatively in the previous section. The second term is positive and hence repulsive. This is the entropic (osmotic) contribution to the force.

At equilibrium, $P_x(D)$ should be uniform throughout the gap—that is, independent of x—and it is also the pressure acting on the two surfaces. To verify this we note that using Eq. (14.7) the above may be written as

$$P_x(D) = kT[\rho_0(D) - \rho_0(\infty)]$$
 (14.17a)

or

$$P_x(D) = kT\rho_0(D)$$
 since here $\rho_0(\infty) = 0$. (14.17b)

which is indeed independent of x and depends only on the increased ionic concentration, or osmotic pressure, at the midplane, $\rho_0(D)$, and thus on σ and D. We may therefore drop the subscript x from $P_x(D)$. It is instructive to insert Eq. (14.8) into the above equation, from which we obtain

$$P(D) = kT\rho_0(D) = kT[\rho_s(D) - \sigma^2/2\varepsilon_0\varepsilon kT],$$

that is,

$$P(D) = kT[\rho_s(D) - \rho_s(\infty)]. \tag{14.18}$$

Thus, the pressure is also given by the increase in the counterion concentration at the surfaces as they approach each other. This important equation, known as the contact value theorem, is always valid as long as there is no interaction between the counterions and the surfaces—that is, as long as there is no counterion adsorption so that the surface coion charge density remains constant and independent of D. It shows that the force or pressure is repulsive if the density of counterions at the surface increases as the two surfaces are brought together and attractive if it decreases.

The contact value theorem is very general and applies to many other types of interactions—for example, to double-layer interactions when electrolyte ions are present in the solution, to solvation interactions where $\rho_s(D)$ is now the surface concentration of solvent molecules (Chapter 15), to polymer-associated steric and depletion interactions where $\rho_s(D)$ is the surface concentration of polymeric groups (Chapter 16), and to various entropic or thermal fluctuation forces between fluid surfaces and biological membranes (Chapters 16 and 21). In the case of overlapping double-layers, the resulting force is often referred to as the *electric* or *electrostatic* double-layer force, even though, as we have seen, the repulsion is really due to entropic confinement.

Returning to Eq. (14.17b), the pressure may also be expressed in terms of K, as given by Eq. (14.11), by

$$P = kT\rho_0 = 2\varepsilon_0 \varepsilon (kT/ze)^2 K^2. \tag{14.19}$$

As an example let us apply this result to Worked Example 14.2, where for two surfaces with $\sigma = 0.2$ C m⁻² at D = 2 nm apart, we found $K = 1.336 \times 10^9$ m⁻¹. The repulsive pressure between them is therefore 1.7×10^6 N m⁻², or about 17 atm. Note that this repulsion exceeds by far any possible van der Waals attraction at this separation. For a typical Hamaker constant of $A \approx 10^{-20}$ J the van der Waals attractive pressure would be only $A/12\pi D^3 \approx 3 \times 10^4 \text{ N m}^{-2}$ or about 0.3 atm.

The above equations have been used successfully to account for the equilibrium spacings of ionic surfactant and lipid bilayers in water (Cowley et al., 1978). Figure 14.5 shows experimental results obtained for the repulsive pressure between bilayers composed of a mixture of charged and uncharged lipids in water using the Osmotic Pressure Technique (cf. Figures 12.1h and 12.2), together with the theoretical curve based on Eq. (14.19). The agreement is very good down to $D \approx 2$ nm and shows that the effective charge density of the anionic lipid headgroups is about 1e per 14 nm². At smaller distances the measured forces are more repulsive than expected due to the sterichydration interactions between the thermally mobile hydrophilic headgroups that characterize these fluid-like interfaces (cf. Problem 14.3 and Chapters 15, 16, and 21). Similar methods have been used to measure the repulsive electrostatic forces between

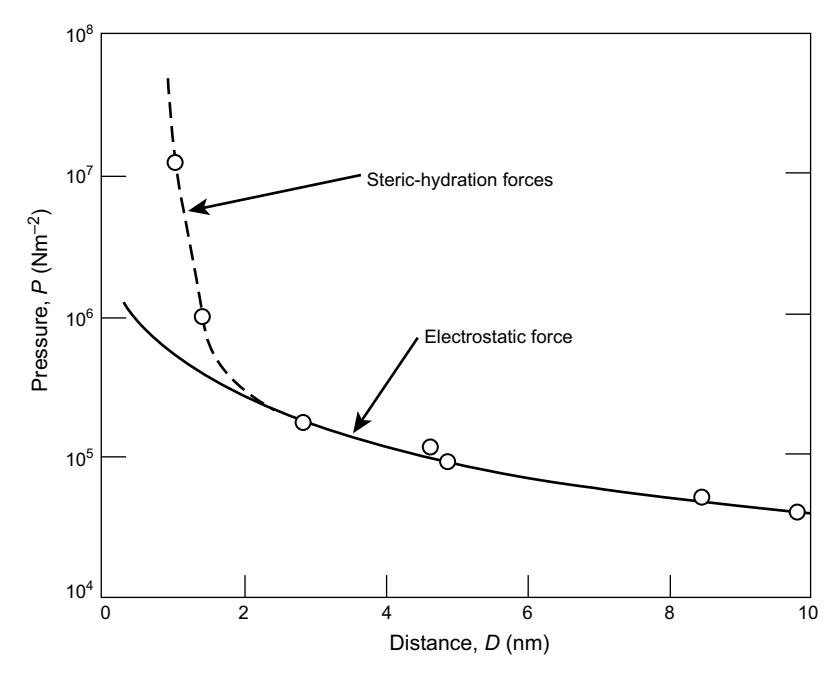


FIGURE 14.5 Measured repulsive pressure between charged bilayer surfaces in water. The bilayers were composed of 90% lecithin (phosphatidylcholine, PC), a neutral zwitterionic lipid, and 10% phosphatidylglycerol (PG), a negatively charged lipid. For full ionization, the surface charge density should be one electronic charge per 7 nm², whereas the theoretical line through the experimental points suggests one charge per 14 nm² (i.e., about 50% ionization). Below 2 nm there is an additional repulsion due to "steric-hydration" forces, [Adapted from Cowlev et al., (1978), ©1978 American Chemical Society.]

surfactant bilayers and biological membranes, both in pure water and in salt solutions (Diederichs et al., 1985; Dubois et al., 1992).

Repulsive electrostatic forces also control the long-range swelling of clays in water. Most naturally occurring clays are composed of lamellar aluminosilicate sheets about 1 to 2 nm thick whose surfaces dissociate in water giving off Na⁺, K⁺, and Ca²⁺ ions, and when placed in water they can swell to more than 10 times their original volume (Norrish, 1954). The swelling of clays is, however, a complex matter and also involves other forces at surface separations below about 3 nm (van Olphen, 1977; Pashley and Quirk, 1984; Kjellander et al., 1988a, b; Quirk, 1994).

In the case of charged spherical particles (e.g., latex particles³) in water, the long-range electrostatic repulsion between them can result in an ordered lattice of particles even when the distance between them is well in excess of their diameter (Takano and Hachisu, 1978). In such systems (cf. Figure 6.2) colloidal particles attempt to get as far apart from each other as possible but, being constrained within a finite volume of solution, are

³Latex particles are made from biological or synthetic polymers. Hydrophobic latex particles can be rendered water-soluble by grafting hydrophilic groups to their surfaces—for example, sulfonic acid groups to polystyrene particles.

forced to arrange themselves into an ordered lattice. For a review on colloidal crystals see Murray and Grier (1996).

Parsegian (1966) and Jönsson and Wennerström (1981) extended the above analysis to the interactions between cylindrical and spherical structures, and the results were used to analyze the relative stability of charged surfactant aggregates which form spontaneously in water. Such micellar structures are soft and fluid-like, and they change from being spherical to cylindrical to sheet-like (bilayers) as the amount of water is reduced (see Chapter 20).

Worked Example 14.3

Question: Two flat but dissimilar surfaces are pressed together with a pressure of 10 atm in pure water (monovalent counterions only, no added electrolyte) at 25°C. If the surfaces carry surface charges of densities $\sigma_1 = -0.04 \text{ C m}^{-2}$ and $\sigma_2 = -0.08 \text{ C m}^{-2}$, respectively, due to the surface dissociation of monovalent surface ions, what will be their equilibrium separation?

Answer: Referring to Figure 14.4 and the equations describing K, the ionic distribution, potential, and pressure for the *symmetrical* case, it is clear that the two halves of the system on either side of the midplane at x = 0 are completely independent of each other as long as ρ_0 and T are fixed (which determine K, ρ_x , ψ_x and P). For the asymmetric case, these same equations apply on either side of the plane at which $E = -d\psi/dx = 0$, which redefines x = 0. All that needs to be done is to find the distance D_1 and D_2 on either side of x=0, where the surface change densities are equal to σ_1 and σ_2 , respectively, as given by Eq. (14.12). Thus, from Eq. (14.19) a pressure of P=10 atm $=1.013\times10^6 \,\mathrm{N\,m^{-2}}$ at $25^{\circ}\mathrm{C}$ corresponds to $K = (ze/kT)\sqrt{P/2\varepsilon_0\varepsilon} = (1.602 \times 10^{-19}/1.381 \times 10^{-23} \times 298.15) \times [(1.013 \times 10^6)/(2 \times 8.854 \times 10^{-19}/1.381 \times 10^{-23} \times 298.15)]$ $10^{-12} \times 78.5$]^{1/2} = 1.05031 $\times 10^9$ m⁻¹. Inserting this value into Eq. (14.12) to get $\frac{1}{2}D$ for $\sigma_1 = -0.04$ and $\sigma_2 = -0.08$ C m⁻² gives $\frac{1}{2}D_1 = 0.78$ nm and $\frac{1}{2}D_2 = 1.08$ nm, respectively. The separation is therefore $D = \frac{1}{2}D_1 + \frac{1}{2}D_2 = 1.86$ nm.

14.8 Limit of Large Separations: Thick Wetting Films

At large distances $D \to \infty$, in order to keep tan(KD/2) finite in Eq. (14.12b), K must approach π/D . In this limit the pressure, Eq. (14.19), therefore becomes

$$P(D) = 2\varepsilon_0 \varepsilon (\pi kT/ze)^2/D^2, \qquad (14.20)$$

that is,

$$P(D) \propto + 1/D^2$$
,

which is known as the Langmuir equation. The Langmuir equation has been used to account for the equilibrium thickness of thick wetting films of water on glass surfaces (Figures 12.1f and 14.6). Here the water-air surface replaces the midplane of Figure 14.2 so that for a film of thickness d = D/2, we have

$$P(d) = \varepsilon_0 \varepsilon (\pi kT/ze)^2 / 2d^2, \tag{14.21}$$

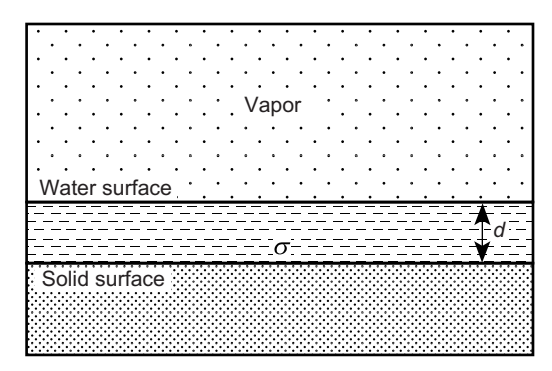


FIGURE 14.6 A water film on a charged (ionizable) glass surface will tend to thicken because of the repulsive "disjoining pressure" of the counterions in the film. If the vapor over the film is saturated, the film will grow indefinitely, but if it is unsaturated, the equilibrium thickness d will be finite as given by Eqs. (14.21) and (14.22).

which is sometimes referred to as the *disjoining pressure* of a film. This repulsive pressure is entirely analogous to the repulsive van der Waals force across adsorbed liquid films, such as helium (Section 13.9), that causes them to climb up or spread on surfaces. Note, however, that both the magnitude and range of the double-layer repulsion is usually greater than the van der Waals' $(P \propto 1/d^2 \text{ instead of } P \propto 1/d^3)$.

In Section 13.9 we saw that the equilibrium thickness d of a wetting film is given by one or other of the following equivalent equations

$$P(d) = +mgH/v = -(kT/v)\log(p/p_{sat}),$$
 (14.22)

where H is the height of the film above the surface of the bulk liquid, v and m the molecular volume and mass of the solvent $(\rho = m/v)$, and p/p_{sat} the relative vapor pressure. Thus, if water condenses on a charged surface from undersaturated vapor, the film thickness d will increase to infinity as H approaches zero or, equivalently, as papproaches p_{sat} (100% relative humidity).

Langmuir (1938) first applied Eq. (14.21) to explain the then paradoxical "Jones-Ray Effect," where the rise of water up a capillary tube is observed to be higher than expected from the Laplace Equation (Chapter 17). Langmuir's explanation was that since the water also wets the inner surface of the capillary, the effective radius of the tube is smaller than the dry radius, and this leads to the higher capillary rise.

Derjaguin and Kusakov (1939) measured how the thickness of a water film on a quartz glass surface decreased when an air bubble was progressively pressed down on the film. The results were in rough agreement with the Langmuir equation. Read and Kitchener (1969) repeated these measurements and again found only rough agreement between theory and experiment: in the range 30-130 nm the measured film thicknesses were 10-20 nm thicker than expected theoretically. Later, Derjaguin and Churaev (1974), Pashley and Kitchener (1979), and Gee et al., (1990b) used the vapor pressure control method to measure the equilibrium film thickness and found that for d < 30 nm the films are much thicker than expected from Eq. (14.22). These effects are believed to be due to one or both of the following: (1) The air-water and hydrocarbon-water interfaces are known to be negatively charged due to the preferential accumulation of OH⁻ ions or depletion of H₃O⁺ ions at these interfaces (Taylor and Wood, 1957; Usui et al., 1981; Marinova et al., 1996; Beattie, 2007), so that for a given disjoining pressure P or vapor pressure p the film thickness would indeed be higher than given by Eq. (14.21), which assumes $\sigma = 0$ and $d\psi/dx = 0$ at that interface; and/or (2) the presence of even small amounts of soluble contaminants in the films will lower p_{sat} in Eq. (14.22), which will result in a large increase in the thickness of the film at any given value of p (Pashley, 1980).

Worked Example 14.4

Problem 3.7 after fragmentation in an atmosphere of relative humidity $p_{\text{vap}}/p_{\text{sat}} = 50\%$ at 20°C? **Answer:** The surface tension or energy of a surface γ is defined by the isothermal work done on changing the area of the surface: $dG = \gamma dA$. For a water droplet with a net charge Q uniformly distributed on its surface, $G = 4\pi R^2 \gamma_0 + Q^2/8\pi \epsilon_0 R$, where γ_0 is the surface tension of pure water ($\gamma_0 = 73 \times 10^{-3} \text{ N m}^{-1}$ at T = 293 K), and $A = 4\pi R^2$ is the surface area. This gives $\gamma = \gamma_0 (1 - Q^2/64\pi^2 \epsilon_0 \gamma_0 R^3)$. At thermodynamic equilibrium, the Laplace pressure of the droplet, given by Eq. (17.15): $P = 2\gamma/R$, equals the pressure of the undersaturated vapor, given by Eq. (14.22): $P = -(RT/V)\log(p_{\text{vap}}/p_{\text{sat}})$, where V = 18 ml is the molar volume of water.⁴ When there is only one charge left per droplet, Q = e, the average equilibrium radius of each droplet will therefore be $(8.3 \times 293/18 \times 10^{-6})\log_e 0.5 = -9.4 \times 10^7 = 2 \times 0.073[1 - (1.602 \times 10^{-6})\log_e 0.5] = -9.4 \times 10^{-6}$ $(10^{-19})^2/(64\pi^2 \times 8.854 \times 10^{-12} \times 0.073R^3)/R$, which is satisfied by R = 0.37 nm, corresponding to a droplet containing about 6 water molecules around the ion.

Question: What are the thermodynamic equilibrium radii of the charged water droplets of

Limit of Small Separations: Osmotic Limit 14.9 and Charge Regulation

At small separations, as $D \to 0$, it is easy to verify from Eq. (14.12) that $K^2 \to -\sigma ze/\varepsilon_0 \varepsilon kTD$ (note that K^2 is positive since σ and z must have opposite signs). Thus, the repulsive pressure P of Eq. (14.19) approaches infinity according to

$$P(D \to 0) = -2\sigma kT/zeD. \tag{14.23}$$

From Eqs. (14.13) and (14.11) we further find that as $D \to 0$ the counterion density profile between the surfaces becomes uniform and equal to

$$\rho_x \approx \rho_s \approx \rho_0 \approx -2\sigma/zeD$$
 at all x . (14.24)

Since $-2\sigma/zeD$ is the number density of counterions in the gap, this means that the limiting pressure of Eq. (14.23) is simply the osmotic pressure $P = \rho kT$ of an ideal gas at

⁴For water, based on molar parameters, $R/V = 8.3/18 \times 10^{-6} = 4.6 \times 10^5 \text{ N m}^{-2} \text{ K}^{-1}$. This can also be expressed in terms of molecular parameters: $k/\nu = 1.38 \times 10^{-23}/30 \times 10^{-30} \text{ N m}^{-2} \text{ K}^{-1}$.

the same density as the trapped counterions. This is known as the *osmotic limit*, which applies to any system where ions, atoms, or molecules remain confined or trapped between two surfaces as they approach each other. In the present case the trapping is due to the requirement of maintaining electroneutrality in the gap that prevents the counterions from going into the surrounding bulk liquid reservoir; in other cases it may be due to the covalent attachment of, for example, polymer molecules to the surfaces. Yet in other cases the trapped molecules may indeed leave the gap, in which case the density ρ is not proportional to 1/D and the resulting pressure can be repulsive, attractive, or oscillatory, as discussed in later chapters.

The infinite pressure as $D \to 0$ implied by Eq. (14.23) is, of course, unrealistic and arises from the assumption that the total number of ions in the gap does not change—that is, that $\sigma = \text{constant}$, which further implies that the surfaces remain fully ionized even when there is a very large pressure pushing the counterions back against the surfaces. In practice when two surfaces are finally forced into molecular contact the counterions are forced to readsorb onto their original surface sites. Thus, as D approaches zero the surface charge density σ also falls—that is, σ becomes a function of D. This is known as *charge regulation*, and its effect is to reduce the repulsion below that calculated on the assumption of constant surface charge. Charge regulation can also arise at isolated surfaces from changes in the solution conditions (rather than from a change in D). These two mechanisms are interdependent and are discussed further in Section 14.17. In addition, other effects and forces can also come in at small separations, and these can be equally important in determining the short-range and especially the adhesion forces at contact.

14.10 Charged Surfaces in Electrolyte Solutions

It is far more common for charged surfaces or particles to interact across or in a solution that already contains electrolyte ions (dissociated inorganic salts). In animal fluids, ions are present in concentrations of about 0.2 M, mainly NaCl or KCl with smaller amounts of MgCl₂ and CaCl₂. The oceans have a similar relative composition of these salts but at a higher total concentration, about 0.6 M. Note that even "pure water" at pH 7 is strictly an electrolyte solution containing 10^{-7} M of H_3O^+ and OH^- ions, which cannot always be ignored. For example, for a charged isolated surface exposed to a solvent containing no added electrolyte ions (only the counterions), Eqs. (14.9) and (14.12) readily show that for the isolated surface, for which $D \to \infty$, we obtain $KD \to \pi$ and $\psi_s \to \infty$. As we shall see, this unrealistic situation is removed as soon as the bulk solvent contains even the minutest concentration of electrolyte ions.

The existence of a "bulk reservoir" of electrolyte ions has a profound effect not only on the electrostatic potential but also on the forces between charged surfaces, and in the rest of this chapter we shall consider this interaction as well as the total interaction when the ever-present van der Waals force is added. But to understand the double-layer interaction between two surfaces it is necessary to first understand the ionic distribution adjacent to an isolated surface in contact with an electrolyte solution. Consider an isolated surface, or

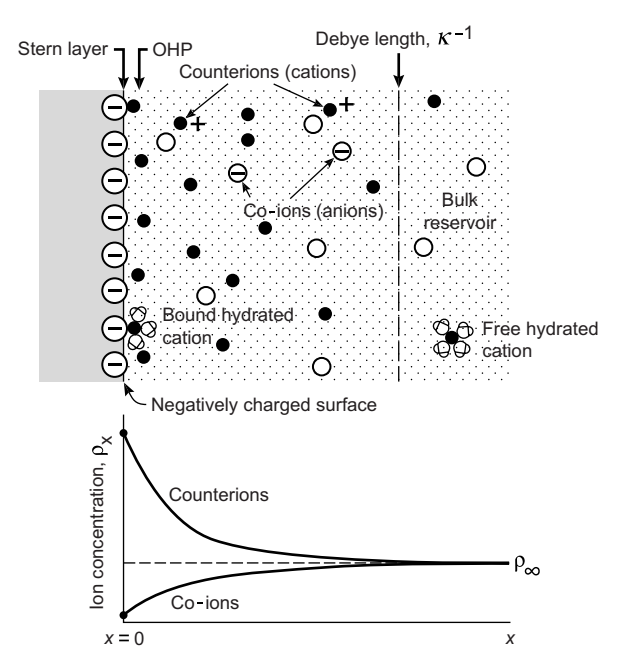


FIGURE 14.7 Near a negatively charged surface there is an accumulation of counterions (ions of opposite charge to the surface coions) and a depletion of coions, shown graphically below for a 1:1 electrolyte, where ρ_{∞} is the electrolyte concentration in the bulk or "reservoir" at $x = \infty$. Counterions can adsorb to the surface in the dehydrated, partially hydrated, or fully hydrated state. The OHP is the plane beyond which the ions obey the Poisson-Boltzmann equation. This plane is usually farther out than the van der Waals plane.

two surfaces far apart, in an aqueous electrolyte (Figure 14.7). For convenience, we shall put x = 0 at the surface rather than at the midplane. Now, all the fundamental equations derived in the previous sections are applicable to solutions containing different types of ions i (of valency z_i) so long as this is taken into account by expressing the net charge density at any point x as $\sum z_i e \rho_{xi}$ and the total ionic concentration (number density) as $\sum \rho_{xi}$. Thus, Eq. (14.2) for the Boltzmann distribution of ions i at x now becomes.

$$\rho_{xi} = \rho_{\infty i} e^{-z_i e \psi_x / kT} \tag{14.25}$$

while at the surface, at x = 0, the contact values of ρ and ψ are related by

$$\rho_{0i} = \rho_{\infty i} e^{-z_i e \psi_0 / kT}, \tag{14.26}$$

where $\rho_{\infty i}$ is the ionic concentration of ions *i* in the bulk (at $x = \infty$) where $\psi_{\infty} = 0$. For example, if we have a solution containing $H^+OH^- + Na^+Cl^- + Ca^{2+}Cl_2^-$, etc., we may write

where [Na⁺], and so on are expressed in some convenient concentration unit such as M (1 M = 1 mol dm⁻³ and corresponds to a number density of $\rho = 6.022 \times 10^{26}$ m⁻³).

14.11 The Grahame Equation

Let us now find the total concentration of ions at an isolated surface of charge density σ . From Eq. (14.8) this is immediately given by

$$\sum_{i} \rho_{0i} = \sum_{i} \rho_{\infty i} + \sigma^{2}/2\varepsilon_{0}\varepsilon kT \qquad \text{(in number per m}^{3}\text{)}. \tag{14.28}$$

Thus, for $\sigma = -0.2$ C m⁻² (corresponding to one electronic charge per 0.8 nm² or 80Å²) at 25°C, we find $\sigma^2/2\varepsilon_0\varepsilon kT = 7.0 \times 10^{27} \,\mathrm{m}^{-3} = 11.64 \,\mathrm{M}$. For a 1:1 electrolyte such as NaCl, the surface concentration of ions in this case is

$$[Na^+]_0 + [Cl^-]_0 = 11.64 + [Na^+]_\infty + [Cl^-]_\infty = 11.64 + 2[Na^+]_\infty = 11.64 + 2[NaCl] \, M, \quad (14.29a)$$
 while for a 2:1 electrolyte such as CaCl₂,

$$[Ca^{2+}]_0 + [Cl^-]_0 = 11.64 + [Ca^{2+}]_{\infty} + [Cl^-]_{\infty} = 11.64 + 3[Ca^{2+}]_{\infty} = 11.64 + 3[CaCl_2] M, \tag{14.29b}$$

where [NaCl] and [CaCl₂] are the bulk molar concentrations of the salts. The ions at the surface are, of course, mainly the counterions (e.g., Na⁺ or Ca²⁺ at a negatively charged surface) and their excess concentration at the surface over that in the bulk is seen to be (1) dependent solely on the surface charge density σ —that is, independent of the bulk electrolyte concentration—and (2) of magnitude sufficient to balance much of the surface charge (cf. Sections 14.4 and 14.15).

We may now find the relation between the surface charge density σ and the surface potential ψ_0 . Incorporating Eq. (14.26) into Eq. (14.28), we obtain for the case of a mixed NaCl + CaCl₂ electrolyte:

$$\sigma^{2} = 2\varepsilon_{0}\varepsilon kT \left(\sum_{i} \rho_{0i} - \sum_{i} \rho_{\infty i}\right)$$

$$= 2\varepsilon_{0}\varepsilon kT \{[\mathrm{Na}^{+}]_{\infty} e^{-e\psi_{0}/kT} + [\mathrm{Ca}^{2+}]_{\infty} e^{-2e\psi_{0}/kT} + [\mathrm{Cl}^{-}]_{\infty} e^{+e\psi_{0}/kT} - [\mathrm{Na}^{+}]_{\infty} - [\mathrm{Ca}^{2+}]_{\infty} - [\mathrm{Cl}^{-}]_{\infty}\}.$$

On further noting that $[Cl^-]_{\infty} = [Na^+]_{\infty} + 2[Ca^{2+}]_{\infty}$ the above becomes

$$\sigma^2 \, = \, 2 \epsilon_0 \epsilon kT \{ [Na^+]_\infty (e^{-e\psi_0/kT} + e^{+e\psi_0/kT} - 2) + [Ca^{2+}]_\infty (e^{-2e\psi_0/kT} + 2e^{+e\psi_0/kT} - 3) \},$$

so that finally we obtain the Grahame equation (Grahame, 1953)

$$\begin{split} \sigma &= \sqrt{8\varepsilon_0\varepsilon kT} sinh(e\psi_0/2kT) \{ [\mathrm{Na^+}]_\infty + [\mathrm{Ca^{2+}}]_\infty (2 + e^{-e\psi_0/kT}) \}^{1/2} \\ &= 0.117 sinh(\psi_0/51.4) \{ [\mathrm{NaCl}] + [\mathrm{CaCl_2}]_\infty (2 + e^{-\psi_0/25.7}) \}^{1/2} \ \mathrm{C\ m^{-2}} \end{split} \tag{14.30}$$

at 25°C, where the bulk concentrations $[NaCl] = [Na^+]_{\infty}$ and $[CaCl_2] = [Ca^{2+}]_{\infty}$ are in M, ψ_0 in mV, and σ in C m⁻² (1 C m⁻² corresponds to one electronic charge per 0.16 nm² or

 16Å^2). For example, a surface having a typical potential of -75 mV in, say, physiological saline solution (150 mM NaCl) has a surface charge density of $\sigma = 0.117 \sqrt{0.150}$ $\sinh(-75.0/51.4) = -0.0922 \text{ C m}^{-2}$. Thus, each charge occupies $0.16/0.092 \approx 1.7 \text{ nm}^2$ or ~170Å², the mean separation between charges on the surface being about 13Å. Equation (14.30) allows us to calculate σ once ψ_0 is known, or vice versa, from which the individual counterion concentrations at each surface ρ_{0i} can be obtained using Eqs. (14.26) or (14.27). We shall now consider some implications of the *Grahame equation*, bearing in mind that it does not *predict* σ or ψ_0 , but just relates them.

Surface Charge and Potential of 14.12 **Isolated Surfaces**

For an aqueous 1:1 electrolyte solution such as NaCl against a negatively charged surface of $\sigma = -0.2 \text{ C m}^{-2}$, we obtain the potentials shown in the middle column of Table 14.1. Note that for no electrolyte we obtain an infinite potential, which is unrealistic; a pure liquid such as water will always contain some dissociated ions. It is for this reason that we did not consider an isolated surface in the absence of bulk electrolyte ions in Section 14.5. From Table 14.1 we find that at constant surface charge density the surface potential falls progressively as the electrolyte concentration rises. From the tabulated values of ψ_0 we can determine the ionic concentrations at the surface using Eq. (14.27). For example, in 10^{-7} M 1:1 electrolyte, where $\psi_0 \approx -477.1$ mV, we obtain $10^{-7} \times e^{+477.1/25.69} = 11.64$ M for the counterions, and $10^{-7} \times e^{-477.1/25.69} \approx 10^{-15}$ M for the coions. In 1 M, where $\psi_0 = -67.0$ mV, we obtain 13.57 M and 0.07 M for the counterions and coions, respectively, which total 13.64 M. As expected, the total concentration of all the ions at the surface agrees exactly with that predicted by Eq. (14.29).

In most cases neither σ nor ψ_0 remains constant as the solution conditions change. This is because ionizable surface sites are rarely fully dissociated but are partially neutralized by the binding of specific ions from the solution. Such ions or surfaces are

Table 14.1	Variation of Surface Potential with Aqueous Electrolyte
Concentrati	on for a Planar Surface of Charge Density $-0.2 \mathrm{C m^{-2}}$ as
Deduced fro	om the Grahame Equation, Eq. (14.30).

	ψ_0 ((mV)
1:1 Electrolyte Concentration (M)	Pure 1:1 Electrolyte Solution	Bulk Solution Also Contains 3 mM 2:1 Electrolyte
0 (hypothetical)		
10^{-7} (pure water)	–477	-106
10^{-4}	-300	-106
10^{-3}	-241	-106
10^{-2}	-181	-105
10^{-1}	-123	-100
1	-67	-66

310

often referred to as *exchangeable* ions or surfaces, in contrast to those *inert* ions that do not bind to the surface. For example, if only protons can bind to a negatively charged surface, the equilibrium condition at the surface is given by the familiar *mass action equation* (Payens, 1955). Thus, for the reaction

$$SH \stackrel{K_d}{\rightleftharpoons} S^- + H^+$$
 at the surface,

where K_d is the surface dissociation constant. We may express the proton concentration at the surface as $[H^+]_0$, the concentration or surface density of negative (dissociated) surface sites as $[S^-]_0$, and the density of neutral (undissociated) sites as $[SH]_0$. The surface charge density σ is related to $[S^-]_0$ via $\sigma = -e[S^-]_0$. Proton concentrations $[H^+]$ are usually given in pH units, defined by pH = $-\log_{10}[H^+]$. The surface dissociation constant K_d is defined by

$$K_{\rm d} = \frac{[S^{-}]_0[H^{+}]_0}{[SH]_0}$$
 (14.31)

$$= \frac{\sigma_0 \alpha}{\sigma_0 (1 - \alpha)} [H^+]_0 = \frac{\alpha}{(1 - \alpha)} [H^+]_{\infty} e^{-e\psi_0/kT}, \qquad (14.32)$$

where σ_0 is the maximum possible charge density (i.e., if all the sites were dissociated) and α is the fraction of sites actually dissociated.

Another important property of an ionizable surface is its pK value, which is the *bulk* pH⁵ at which half of its charged sites are dissociated ($\alpha=0.5$). At this point Eq. (14.32) shows that $K_{\rm d}=[{\rm H}^+]_{\infty}e^{-e\psi_0/kT}$. Thus, the pK can be directly equated with the dissociation constant. For example, if half the sites are dissociated at $[{\rm H}^+]_{\infty}=[{\rm H}^+]_{\infty}^{pK}=10^{-4}$ M (pH 4.0), we would say that the pK of the surface is 4.0. If both $K_{\rm d}$ and ψ_0 remain constant as the pH changes, then at any different $[{\rm H}^+]_{\infty}$ or pH the fraction of dissociated sites can be written as

$$\alpha = \frac{K_{\rm d}}{K_{\rm d} + [{\rm H}^+]_{\infty} e^{-e\psi_0/kT}} = \frac{[{\rm H}^+]_{\infty}^{pK}}{[{\rm H}^+]_{\infty}^{pK} + [{\rm H}^+]_{\infty}} = \frac{10^{-4}}{10^{-4} + [{\rm H}^+]_{\infty}}.$$
 (14.33)

Thus, at pH 3 (corresponding to ten times the proton concentration at the pK) we find $\alpha = 0.09$, while at pH 5 (ten times lower proton concentration) we find $\alpha = 0.91$.

For a mixed 1:1 electrolyte consisting of inert (non-surface-binding) and surface-binding H^+ ions—for example, a mixture of NaCl and HCl—Eq. (14.32) can be combined with the Grahame equation to give the simultaneous equations

$$\sigma = \alpha \sigma_0 = K_{\rm d} \sigma_0 / (K_{\rm d} + [\rm HCl]_{\infty} e^{-\psi_0 / 25.7}) = 0.117 \sinh(\psi_0 / 51.4) \sqrt{[\rm NaCl]_{\infty} + [\rm HCl]_{\infty}}$$
 (14.34)

in which both σ and ψ_0 can now be totally determined in terms of the maximum charge density σ_0 and dissociation constant K_d . It is clear from the above that if K_d is very

⁵Note that if the pH is defined in terms of the concentration (number density) of protons, then the surface pH of $-\log_{10}[H^+]_0$ is different from the bulk pH of $-\log_{10}[H^+]_\infty$. However, if the pH is defined in terms of the *activity* of the protons, the two values are identical, since they are now being equated with the chemical potential of the protons.

large (high surface charge, weak binding of protons), then $\sigma \approx \sigma_0 \approx \text{constant}$, and we obtain the earlier result for the case of fixed surface charge density. However, if K_d takes on a more typical value, the effect can be quite dramatic. For example, if $K_d = 10^{-4}$ M, then for a surface of $\sigma_0 = -0.2 \text{ C m}^{-2}$ in a 0.1 M NaCl bulk solution at pH 7, we find $\psi_0 =$ -118 mV and $\alpha = 0.91$ —that is, the protons have neutralized 9% of the surface sites, and ψ_0 is not very different from the value in the absence of protons (see Table 14.1). But at pH 5 we obtain $\psi_0 = -73$ mV and $\alpha = 0.36$ —that is, only 36% of the sites now remain dissociated even though the bulk concentration of HCl is a mere 0.01% of the NaCl concentration. Under such conditions the proton is referred to as a potential determining ion. Thus, both ψ_0 and σ will vary as the salt concentration or pH is changed, but the surface will always remain negatively charged.

More generally, a surface may contain both anionic (e.g., acidic) and cationic (e.g., basic) groups to which various cations and anions can bind. Such surfaces are known as amphoteric, and the competitive adsorption of ions to them can be analyzed by assigning a binding constant to each ion type, and then incorporating these into the Grahame equation (Healy and White, 1978; Chan et al., 1980a). The charge density of amphoteric surfaces (e.g., protein surfaces) can be negative or positive depending on the electrolyte conditions. At the isoelectric point (iep) or point of zero charge (pzc) there are as many negative charges as positive charges so that the mean surface charge density is zero $(\sigma = 0)$, although it is important to remember that there may still be local regions of high negative or positive charge. Such discrete local charges become crucially important for determining the short-range and adhesion forces between amphoteric surfaces and biological macromolecules, and we return to consider such acid-base and proteinsubstrate interactions in later sections and in Part III.

Effect of Divalent Ions 14.13

The presence of divalent cations has a dramatic effect on the surface potential and counterion distribution at a negatively charged surface. For example, if all the NaCl solutions of Table 14.1 also contain 3×10^{-3} M CaCl₂, the Grahame equation gives the potentials shown in the third column. We see that even at constant surface charge density, relatively small amounts of divalent ions substantially lower the magnitude of ψ_0 , in fact, about 100 times more effectively than increasing the concentration of monovalent salt. Indeed, ψ_0 is determined solely by the divalent cations once their concentration is greater than about 3% of the monovalent ion concentration, and for 2:1 electrolyte concentrations above a few mM, typical surface potentials are well below -100 mV irrespective of the 1:1 electrolyte concentration.

Further, even when the bulk concentration of Ca²⁺ is much smaller than that of Na⁺, the surface may have a much higher local concentration of Ca²⁺. For example, in 100 mM NaCl + 3 mM CaCl₂, where $\psi_0 = -100$ mV (see Table 14.1) the concentration of Ca²⁺ at the surface is $[Ca^{2+}]_0 \approx 3 \times 10^{-3} e^{+200/25.7} \approx 7$ M compared to $[Na^+]_0 \approx 0.1 e^{+100/25.7} \approx 5$ M. At such high surface concentrations (of *doubly* charged ions) divalent ions often bind chemically to negative surface sites, thereby lowering σ and reducing ψ_0 even further, and it is not unusual for surfaces to be completely neutralized ($\sigma \to 0$, $\psi_0 \to 0$) in the presence of mM amounts of Ca²⁺. In the case of trivalent ions such as La³⁺, bulk concentrations in excess of 10^{-5} M can neutralize a negatively charged surface and even lead to *charge reversal* wherein the cations continue to adsorb onto a surface that is already net positively charged (see Problem 3. 2(ii)).

As in the case of monovalent ion binding, the effect of divalent ion binding can be dealt with quantitatively by incorporating the appropriate binding constants into the Grahame equation (Healy and White, 1978; McLaughlin et al., 1981), and when many different ionic species (e.g., Ca^{2+} , H^+) compete for binding sites the variation of ψ_0 and σ with electrolyte concentration and pH can be quite complex. In most cases ion binding tends to lower both σ and ψ_0 as the concentrations of these ions increase, and we may anticipate that such effects lead to a substantial reduction in the repulsive double-layer forces between surfaces.

14.14 The Debye Length

For low potentials, below about 25 mV, the Grahame equation simplifies to

$$\sigma = \varepsilon_0 \varepsilon \kappa \psi_0, \tag{14.35}$$

where

$$\kappa = \left(\sum_{i} \rho_{\infty i} e^{2} z_{i}^{2} / \varepsilon_{0} \varepsilon kT\right)^{1/2} \mathbf{m}^{-1}.$$
 (14.36)

Thus, the potential becomes proportional to the surface charge density. Equation (14.35) is the same as Eq. (14.14) for a capacitor whose two plates are separated by a distance $1/\kappa$, have charge densities $\pm \sigma$, and potential difference ψ_0 . This analogy with a charged capacitor gave rise to the name *diffuse electric double-layer* for describing the ionic atmosphere near a charged surface, whose characteristic length or "thickness" is known as the Debye length, $1/\kappa$.

The magnitude of the Debye length depends solely on the properties of the solution and not on any property of the surface such as its charge or potential. For a monovalent electrolyte (z=1) at 25°C (298K) the Debye length of aqueous solutions is

$$\kappa^{-1} = (\varepsilon_0 \varepsilon kT/2 \rho_\infty e^2)^{1/2} = \left(\frac{8.854 \times 10^{-12} \times 78.4 \times 1.381 \times 10^{-23} \times 298}{2 \times 6.022 \times 10^{26} \times (1.602 \times 10^{-19})^2 M}\right)^{1/2} = 0.304 \times 10^{-9}/\sqrt{M} \text{ m}.$$

Thus,

$$\begin{array}{lll} & 0.304/\sqrt{[\text{NaCl}]} \text{ nm} & \text{for 1:1 electrolytes (e.g., NaCl)} \\ 1/\kappa = & 0.176/\sqrt{[\text{CaCl}_2]} \text{ nm} & \text{for 2:1 and 1:2 electrolytes (e.g., CaCl}_2, \text{ Na}_2\text{SO}_4) \\ & 0.152/\sqrt{[\text{MgSO}_4]} \text{ nm} & \text{for 2:2 electrolytes (e.g., MgSO}_4) \end{array} \tag{14.37}$$

For example, for NaCl solution, $1/\kappa = 30.4$ nm at 10^{-4} M, 9.6 nm at 1 mM, 0.96 nm at 0.1 M, and 0.3 nm at 1 M. In totally pure water at pH 7, the Debye length is 960 nm, or about 1 µm.

Variation of Potential ψ_x and Ionic 14.15 Concentrations ρ_x Away from a Surface

The potential gradient at any distance x from an isolated surface is given by Eq. (14.7):

$$\sum_{i} \rho_{xi} = \sum_{i} \rho_{\infty i} + \frac{\varepsilon_0 \varepsilon}{2kT} \left(\frac{\mathrm{d}\psi}{\mathrm{d}x}\right)_{x}^{2}.$$
 (14.38)

For a 1:1 electrolyte this gives

$$\mathrm{d}\psi/\mathrm{d}x = \sqrt{8kT\rho_{\infty i}/\varepsilon_0\varepsilon} \sinh(e\psi_x/2kT),$$

which may be readily integrated using the integral $\left[\operatorname{csch}X dX = \log \tanh(X/2)\right]$ to yield

$$\psi_{x} = \frac{2kT}{e} \log \left[\frac{1 + \gamma e^{-\kappa x}}{1 - \gamma e^{-\kappa x}} \right] \approx \frac{4kT}{e} \gamma e^{-\kappa x}, \tag{14.39}$$

where⁶

$$\gamma = \tanh(e\psi_0/4kT) = \tanh[\psi_0(mV)/103] \text{ at } 25^{\circ}\text{C}.$$
 (14.40)

This is known as the *Gouy-Chapman* theory. For high potentials $\gamma \to 1$, while for potentials less than 25 mV, Eq. (14.39) reduces to the so-called *Debye-Hückel* equation

$$\psi_{x} \approx \psi_{0} e^{-\kappa x},\tag{14.41}$$

where again the Debye length $1/\kappa$ appears as the characteristic decay length of the potential [see Verwey and Overbeek (1948) and Hiemenz (1997) for a fuller discussion of the Gouy-Chapman and Debye-Hückel theories].

The above equations apply to *symmetrical* 1:1 electrolyte solutions, such as NaCl. Equations that apply to asymmetrical electrolytes—for example, 2:1 and 1:2 electrolytes such as CaCl₂ and Na₂SO₄—have been derived by Grahame (1953). These are more complicated than Eq. (14.39), but for low ψ_0 they all reduce to $\psi_x = \psi_0 e^{-\kappa x}$.

We now have all the equations needed for computing the ionic distributions away from a charged surface. For a 1:1 electrolyte, this is given by inserting Eq. (14.39) into Eq. (14.25) or (14.27). Figure 14.8 shows the variation of ψ_x and ρ_x for a 0.1 M 1:1 electrolyte, together with a Monte Carlo simulation for comparison. Note how the counterion density approaches the bulk value much faster than would be indicated by the Debye length. Indeed, for such a high surface charge density and potential the counterion distribution very near the surface is largely independent of the bulk electrolyte concentration, and it is left as an exercise for the reader to verify that even in 10^{-4} M the counterion profile over the first few angstroms is not much different from that in 0.1 M (so long as σ remains the same).

⁶ tanh $x = (e^x - e^{-x})/(e^x + e^{-x})$.

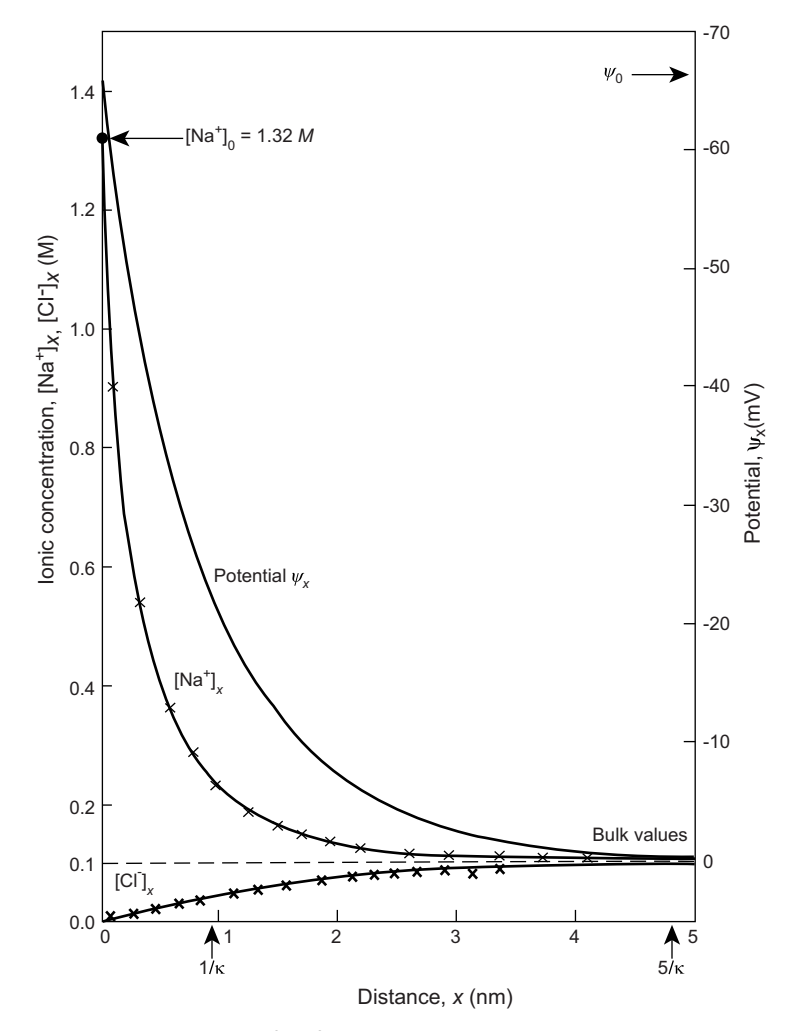


FIGURE 14.8 Potential and ionic density profiles for a 0.1 M monovalent electrolyte such as NaCl near a surface of charge density $\sigma = -0.0621 \, \text{C m}^{-2}$ (about one electronic charge per 2.6 nm²), calculated from Eqs. (14.39) and (14.25) with $\psi_0 = -66.2$ mV obtained from the Grahame equation. The crosses are the Monte Carlo results of Torrie and Valleau (1979, 1980). Note that the potential (and force between two surfaces) both decay asymptotically as $e^{-\kappa x}$, while the ionic concentrations decay much more sharply.

14.16 **Electrostatic Double-Layer Interaction Forces** and Energies between Various Particle Surfaces

The interaction pressure between two identically charged surfaces in an electrolyte solution (Figure 14.9) can be derived quite simply as follows. First, from Section 14.7 we note that at any point x the pressure $P_x(D)$ is given by

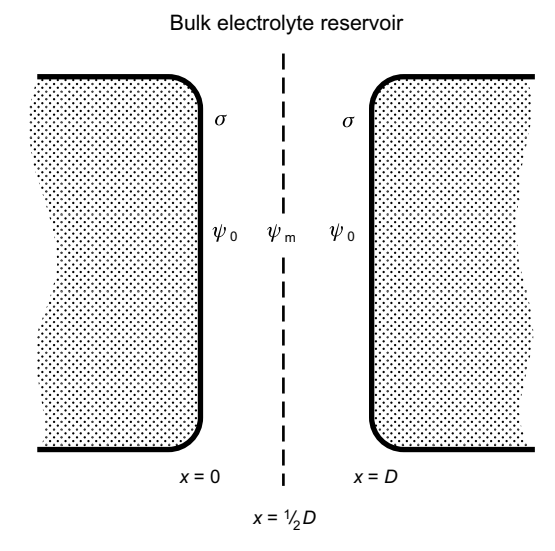


FIGURE 14.9

$$P_{x}(D) - P_{x}(\infty) = -\frac{1}{2} \varepsilon_{0} \varepsilon \left[\left(\frac{\mathrm{d}\psi}{\mathrm{d}x} \right)_{x(D)}^{2} - \left(\frac{\mathrm{d}\psi}{\mathrm{d}x} \right)_{x(\infty)}^{2} \right] + kT \left[\sum_{i} \rho_{xi}(D) - \sum_{i} \rho_{xi}(\infty) \right]. \tag{14.42}$$

Second, from Eq. (14.7) we have

$$\sum_{i} \rho_{xi} = \sum_{i} \rho_{mi} + \frac{\varepsilon_0 \varepsilon}{2kT} \left(\frac{d\psi}{dx}\right)_{x}^{2}$$
(14.43)

for any x or D, where $\Sigma \rho_{\text{m}i}$ is the total ionic concentration at the midplane at $x = \frac{1}{2}D$. Incorporating Eq. (14.43) into Eq. (14.42), and again putting $P_x(D = \infty) = 0$, yields two useful and equivalent expressions for the pressure:

$$P_{x}(D) = kT \left[\sum_{i} \rho_{0i}(D) - \sum_{i} \rho_{0i}(\infty) \right] = kT \left[\sum_{i} \rho_{mi}(D) - \sum_{i} \rho_{mi}(\infty) \right]$$
(14.44)

which, as before, is the uniform pressure across the gap (independent of position x) acting on the electrolyte ions and on the surfaces. The above result is essentially the same as Eqs. (14.17) and (14.18) and shows that P is simply the excess osmotic pressure of the ions at the surfaces or in the midplane. Since $\Sigma \rho_{mi}(\infty)$ is known from the bulk electrolyte concentration the problem reduces to finding the midplane concentration of ions $\rho_{mi}(D)$ when D is finite, and it is here that certain assumptions have to be made to obtain an analytic result (Verwey and Overbeek, 1948). For a 1:1 electrolyte such as NaCl, Eq. (14.44) may be written as

$$P = kT \rho_{\infty} \left[(e^{-e\psi_{\rm m}/kT} - 1) + (e^{+e\psi_{\rm m}/kT} - 1) \right] = 2kT \rho_{\infty} \left[\cosh(e\psi_{\rm m}/kT) - 1 \right]$$
 cations anions (14.45)

$$\approx e^2 \psi_{\rm m}^2 \rho_{\infty} / kT \quad \text{for } \psi_{\rm m} < 25 \text{ mV}, \tag{14.46}$$

which assumes that the midplane potential $\psi_{\rm m}$ (not the surface potential ψ_0) is small. If we further assume that $\psi_{\rm m}$ is simply the sum of the potentials from each surface at $x=\frac{1}{2}D$ as previously derived for an isolated surface, then Eq. (14.39) gives $\psi_{\rm m} \approx 2(4kT\gamma/e)e^{-\kappa D/2}$. Inserting this into Eq. (14.46) gives the final result for the repulsive pressure between two planar surfaces across a 1:1 electrolyte:

$$P = 64kT\rho_{\infty}\gamma^{2}e^{-\kappa D} = (1.59 \times 10^{8})[\text{NaCl}]\gamma^{2}e^{-\kappa D} \text{ N m}^{-2} \quad \text{at } 25^{\circ}\text{C (298 K)},$$
 (14.47)

where we note that $\gamma = \tanh(ze\psi_0/4kT)$ can never exceed unity. Equation (14.47) is known as the weak overlap approximation or linear superposition approximation (SLA) for the interaction between two similar surfaces at constant potential.

The interaction free energy per unit area corresponding to the above pressure is obtained by a simple integration with respect to D, and gives

$$W_{\text{flats}} = (64kT\rho_{\infty}\gamma^2/\kappa)e^{-\kappa D} \tag{14.48}$$

$$= 0.0482 [\text{NaCl}]^{1/2} \tanh^2 [\psi_0(\text{mV})/103] e^{-\kappa D} \ \text{J m}^{-2} \qquad \text{(for 1:1 electrolytes)} \eqno(14.49)$$

$$= 0.0211 [{\rm MgSO_4}]^{1/2} \tanh^2 [2\psi_0({\rm mV})/103] e^{-\kappa {\rm D}} \ \ {\rm J \ m^{-2}} \qquad ({\rm for \ 2:2 \ electrolytes}), \eqno(14.50)$$

where in the above equations the bulk concentrations [NaCl] and [MgSO₄] are in M. There is no simple expression for 2:1 or 1:2 electrolytes, or for mixed 1:1 and 2:1 electrolytes (Chan, 2002), but it is interesting to note that for surface potentials between 50 and 80 mV the values of 0.0482 $\tanh^2 \left[\frac{\psi_0}{103} \right]$ and 0.0211 $\tanh^2 \left[\frac{2\psi_0}{103} \right]$ differ by less than 20%, suggesting that either of the above equations provides a good approximation so long as the correct Debye length is used (which can always be accurately calculated using Eq. (14.36).

Applying the Derjaguin approximation, Eq. (11.16), we may immediately write the expression for the force F between two spheres of radius R as $F = \pi RW$, from which the interaction free energy is obtained by a further integration (see Sader et al., 1995, for more accurate formulae for spheres):

$$W_{\text{spheres}} = (64\pi kTR\rho_{\infty}\gamma^{2}/\kappa^{2})e^{-\kappa D} = 4.61 \times 10^{-11}R\gamma^{2}e^{-\kappa D} \text{ J}$$
 (for 1:1 electrolytes). (14.51)

We see therefore that the double-layer interaction between surfaces or particles of different geometries always decays exponentially with distance with a characteristic decay length equal to the Debye length. This is quite different from the van der Waals interaction where the decay is a power law having very different exponents for different geometries. Figure 13.1 gave the different expressions for the van der Waals forces and energies between bodies of different geometries in terms of their dimensions and the Hamaker Constant. Figure 14.10 is a similar figure for the double-layer forces and energies, given in terms of the dimensions of the particles, the Debye length κ^{-1} , and an "interaction constant" Z defined by

$$Z = 64\pi\varepsilon_0\varepsilon(kT/e)^2 \tanh^2(ze\psi_0/4kT) \text{ J m}^{-1}\text{or N}$$
(14.52)

$$= (9.22 \times 10^{-11}) \tanh^2(\psi_0/103) \text{ J m}^{-1} \text{ at } 25^{\circ}\text{C or } 298 \text{ K (room temperature)}$$
 (14.53)

$$= (9.38 \times 10^{-11}) \ tanh^2 (\psi_0/107) \ \ J \ m^{-1} \ at \ 37^{\circ}C \ or \ 310 \ K \ (physiological \ temperature) \ \eqno(14.54)$$

Geometry of bodies with surfaces <i>D</i> apart (<i>D</i> « <i>R</i>)		Electric 'Double-layer' Interaction		
		Energy, W	Force, F= -dW/dD	
Two ions or small charged molecules	TWO IONS IN WATER $ z_1 e \bigotimes_{Z \ge e} solvent $ $solvent$	$\frac{+z_1z_2e^2}{4\pi\epsilon_0\epsilon r} \frac{e^{-\kappa(r-\sigma)}}{(1+\kappa\sigma)}$	$\frac{+z_1z_2e^2}{4\pi\varepsilon_0\varepsilon r^2}\frac{(1+\kappa r)}{(1+\kappa\sigma)}e^{-\kappa(r-\sigma)}$	
Two flat surfaces (per unit area)	TWO FLAT SURFACES Area = πα² Area = πα² T ≯ D	$W_{\text{Flat}} = (\kappa / 2\pi) \text{Ze}^{-\kappa D}$	$(\kappa^2/2\pi)Ze^{-\kappa D}$	
Two spheres or macromolecules of radii R_1 and R_2	TWO SPHERES $\begin{array}{c} & & & \\ & \uparrow & & \\ \uparrow & & & \\ D & & & \\ & & & \\ & & & \\ & & & \\ & & & \\ & & & \\ & & & \\ & & & \\ & & & \\ & & & \\ & & & \\ & & & \\ & & & \\ & & & \\ & & & \\ & & & \\ & & & \\ & & \\ & & & \\ & \\ & & \\ & & \\ & & \\ & \\ & & \\ & & \\ & & \\ & & \\ & & \\ & & \\ & & \\ & & \\ & &$	$\left(\frac{R_1 R_2}{R_1 + R_2}\right) Z e^{-\kappa D}$	$\kappa \left(\frac{R_1 R_2}{R_1 + R_2} \right) Z e^{-\kappa D}$ Also $F = 2\pi \left(\frac{R_1 R_2}{R_1 + R_2} \right) W_{\text{Flat}}$	
Sphere or macro- molecule of radius <i>R</i> near a flat surface	SPHERE ON FLAT	RZe ^{−ĸD}	$\kappa R Z e^{-\kappa D}$ Also $F = 2\pi R W_{\text{Flat}}$	
Two parallel cylinders or rods of radii R_1 and R_2 (per unit length)	TWO PARALLEL CYLINDERS	$\frac{\kappa^{1/2}}{\sqrt{2\pi}} \left(\frac{R_1 R_2}{R_1 + R_2} \right)^{1/2} Z e^{-\kappa D}$	$\frac{\kappa^{3/2}}{\sqrt{2\pi}} \left(\frac{R_1 R_2}{R_1 + R_2} \right)^{1/2} Z e^{-\kappa D}$	
Cylinder of radius R near a flat surface (per unit length)	CYLINDER ON FLAT	$\kappa^{1/2} \sqrt{\frac{R}{2\pi}} Z e^{-\kappa D}$	$ \kappa^{3/2} \sqrt{\frac{R}{2\pi}} Z e^{-\kappa D} $	
Two cylinders or filaments of radii R_1 and R_2 crossed at 90°	CROSSED CYLINDERS R ₁ R ₂ R ₁ R ₁ R ₂ D	$\sqrt{R_1R_2}$ Ze ^{-κD}	$\kappa \sqrt{R_1 R_2} \operatorname{Ze}^{-\kappa D}$ Also $F = 2\pi \sqrt{R_1 R_2} W_{\text{Flat}}$	

FIGURE 14.10 Electrostatic double-layer interaction energies W(D) and forces (F = -dW/dD) between similar constant potential surfaces of different geometries in terms of the interaction constant Z defined by Eq. (14.52). For a monovalent 1:1 electrolyte such as NaCl (z=1), $Z=64\pi\epsilon_0\epsilon(kT/e)^2 \tanh^2(e\psi_0/4kT)=(9.22\times 10^{-11} \tanh^2(\psi_0/103)$ J m⁻¹at 25°C and (9.38×10^{-11}) tanh² $(\psi_0/107)$ J m⁻¹ at 37°C (body temperature). The Debye length, κ^{-1} , is defined by Eq. (14.36).

where ψ_0 is in mV. The interaction constant **Z** is analogous to the Hamaker Constant **A**, and-apart from the electrolyte valency z-depends only on the properties of the surfaces. The other terms that appear in the expressions for the interaction energies and forces, such as κ , depend only on the *solution* and on the geometry and separation of the surfaces. Note that the interaction constant Z is defined in terms of the surface potential ψ_0 of the isolated surfaces (at $D=\infty$), but it can also be expressed in terms of the surface charge density σ by applying the Grahame Equation.

As an example of the use of Figure 4.10, the double-layer energy for two identical spheres of radius R is given in the 4th row as $W(D) = Z R_1 R_2 e^{-\kappa D}/(R_1 + R_2) =$ $\frac{1}{2}ZRe^{-\kappa D} = (4.61 \times 10^{-11})R \tanh^2(\psi_0/103)e^{-\kappa D}$ J, which is the same as Eq. (14.51).

It is important to note that with increasing ionic strength, even though the Debye length falls due to the increased screening of the electric field, the asymptotic short-range force or energy can increase, depending on the geometry of the particles. This unintuitive result arises for those geometries in Figure 14.10, where κ appears in the numerator, for example, as occurs for both the energy and force between two planar surfaces. For such systems, as $D \to 0$ and $e^{-\kappa D} \to 1$, the repulsion at constant potential (Z = constant) is seen to increase with increasing ionic strength (increasing κ). This has important implications for the shortrange and adhesion forces in aqueous solutions, as discussed later (cf. Figure 14.15).

At low surface potentials, below about 25 mV, all the above equations simplify to the following: For two planar surfaces,

$$P \approx 2\varepsilon_0 \varepsilon \kappa^2 \psi_0^2 e^{-\kappa D} = 2\sigma^2 e^{-\kappa D} / \varepsilon_0 \varepsilon \text{ N m}^{-2}$$
 (14.55)

and

$$W \approx 2\varepsilon_0 \varepsilon \kappa \psi_0^2 e^{-\kappa D} = 2\sigma^2 e^{-\kappa D} / \kappa \varepsilon_0 \varepsilon \text{ J m}^{-2}$$
 (14.56)

while for two spheres of radius R,

$$F \approx 2\pi R \varepsilon_0 \varepsilon \kappa \psi_0^2 e^{-\kappa D} = 2\pi R \sigma^2 e^{-\kappa D} / \kappa \varepsilon_0 \varepsilon \text{ N}$$
 (14.57)

and

$$W \approx 2\pi R \varepsilon_0 \varepsilon \psi_0^2 e^{-\kappa D} = 2\pi R \sigma^2 e^{-\kappa D} / \kappa^2 \varepsilon_0 \varepsilon \text{ J.}$$
 (14.58)

In the above, ψ_0 and σ are related by $\sigma = \varepsilon_0 \varepsilon \kappa \psi_0$, which, as we have seen, is valid for low potentials. These four equations are quite useful because they are valid for all electrolytes, whether 1:1, 2:1, 2:2, 3:1, or even mixtures as long as the appropriate Debye lengths are used as given by Eqs. (14.36)–(14.37). Thus, they are particularly suitable when divalent ions are present, since the surface charge and potential is often low due to ion binding.

14.17 Exact Solutions for Constant Charge and Constant Potential Interactions: Charge Regulation

All the expressions derived so far are accurate only for surface separations beyond about one Debye length. At smaller separations one must resort to numerical solutions of the Poisson-Boltzmann equation to obtain the exact interaction potential (Verwey and Overbeek, 1948; Devereux and De Bruyn, 1963; Honig and Mul, 1971) for which there are no simple expressions that cover all possible situations. Figures 14.11 and 14.12 show

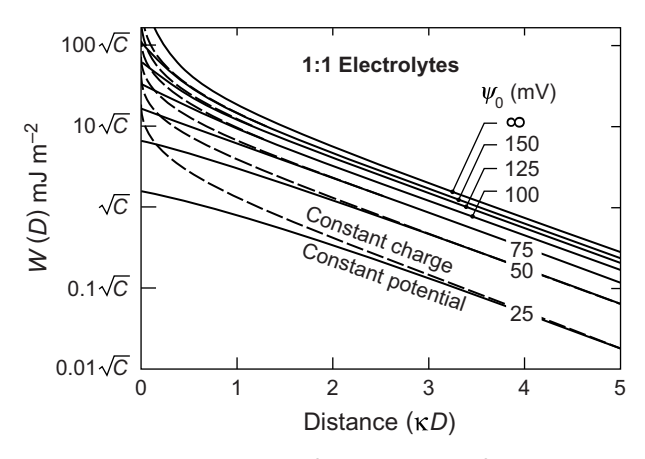


FIGURE 14.11 Repulsive double-layer interaction energy for two planar surfaces in a 1:1 electrolyte [exact solution kindly computed by M. Sculley, R. Pashley, and L. White based on Ninham and Parsegian (1971)]. √₀ is the potential of the isolated surfaces and C the electrolyte concentration in M, which is related to the Debye length by $1/\kappa = 0.304/$ \sqrt{C} nm. Theoretically, the double-layer interaction must lie between the constant-charge and constant-potential limits. (---) constant charge, (—) constant potential. However, these limits are based on the validity of the Poisson-Boltzmann (PB) equation; if other forces, such as ion-correlation, hydrophobic, or steric-hydration, are present, the interaction can be more attractive or more repulsive. At separations greater than $1/\kappa$ the forces and energies are well described by Eqs. (14.47)–(14.51) for z = 1.

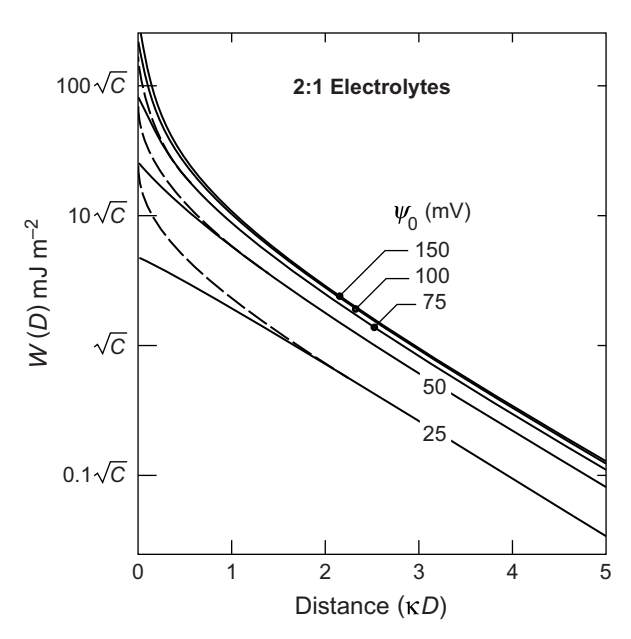


FIGURE 14.12 Repulsive double-layer interaction energy for two planar surfaces in a 2:1 electrolyte where the counterions—that is, the ions of opposite charge to those on the surface—are divalent [computed as in Figure 14.11]. For 1:2 electrolytes (where the counterions are monovalent) the interaction is approximately as for a 1:1 electrolyte but with the Debye length as for a 2:1 or 1:2 electrolyte—that is, Debye length $1/\kappa = 0.176/\sqrt{C}$ nm, where C is the electrolyte concentration in M. (---) constant charge, (—) constant potential. At separations greater than $1/\kappa$ the forces are well described by Eqs. (14.47)–(14.51) for z = 2.

plots of the exact numerical solutions for the double-layer interaction potentials of two planar surfaces in pure 1:1 and 1:2 electrolytes in the two limiting cases of constant charge and constant potential. The figures may be used for reading off the interaction energy of any 1:1 or 2:1 electrolyte at any desired concentration C, and surface separation D. This is because the energy scales with \sqrt{C} and the distance scales with the Debye length, κ^{-1} . The constant potential curves of Figure 14.11 compare reasonably well with the approximate expression of Eq. (14.48) even at small separations, and especially when ψ_0 is between 50 and 100 mV. In contrast, as shown by the dashed curves in Figures 14.11 and 14.12, interactions at constant charge are always greater than those at constant potential, especially at separations below 1-2 Debye lengths where they veer sharply upwards, becoming infinite as $D \to 0$, while the constant potential interaction tends toward a finite value.

In addition there is the question of charge regulation at small separations. In general, neither the surface charge density nor the potential remain constant as two surfaces come close together. Instead, as was discussed in Section 14.9, some of the counterions are forced back onto the surfaces thereby reducing σ . This affects the form of the interaction which now falls between the constant charge and constant potential limits. At large distances, beyond a few κ^{-1} , all the interaction pressures and energies merge and are well described by the equations based on the Linear Superposition Approximation as listed in Figure 14.10.

If there is no binding, the surface charge density remains constant, and in the limit of small D the number density of monovalent counterions between the two surfaces will approach a uniform value of $2\sigma/eD$. From Eq. (14.44) the limiting pressure in this case is

$$P(D \to 0) = kT \sum_{i} \rho_{mi} = -2\sigma kT/zeD = +|2\sigma kT/zeD|, \qquad (14.59)$$

and

$$W(D \to 0) = (-2\sigma kT/ze)\log D + \text{constant}, \tag{14.60}$$

that is, as $D \to 0$ the pressure and the energy become infinite. Note that this is the same osmotic limit as in the case of no bulk electrolyte (counterions only), Eq. (14.23), and results from the limiting osmotic pressure of the "trapped" counterions.

If there is counterion binding as D decreases—that is, charge regulation—P falls below this limit, and the Poisson-Boltzmann equation must now be solved self-consistently by including the dissociation constants of the adsorbing ions (cf. Section 14.12). The computations have been described by Ninham and Parsegian (1971) and Healy et al., (1980), and simple numerical algorithms have been given by Chan et al., (1976, 1980b). So long as the Poisson-Boltzmann equation remains valid, the double-layer forces between two symmetrical charge-regulating surfaces always lie between the constant surface charge and constant surface potential limits shown in Figures 14.11 and 14.12.7 When the PB equation breaks down—for example, when the electrolyte contains multivalent

Although Borkovec and Behrens (2008) have suggested that under certain conditions the double-layer interaction can be weaker than at constant potential.

counterions—or when other forces, such as ion-correlation forces, are present, then the resulting interaction can be very different and even change sign—that is, become attractive. And the situation becomes much more complex for asymmetric surfaces, even in the absence of charge regulation.

An often overlooked feature of a charge-regulating interaction is that as two surfaces approach each other there is a continual exchange of ions with the bulk reservoir. This takes time. If two surfaces are brought together quickly, the interaction may be at constant charge even though the equilibrium interaction is at constant potential (Raviv et al., 2002; Anderson et al., 2010).8 And the issue is not only determined by the diffusion of ions into and out of the interaction zone; quite often the ion exchange processes at the interfaces is slow (minutes) and is the rate-limiting part of the overall interaction.

14.18 **Asymmetric Surfaces**

For two surfaces of different charge densities or potentials the interaction energy can have a maximum or minimum at some finite distance, usually below $1/\kappa$. Approximate equations for the interactions of two surfaces of unequal but constant potentials were given by Hogg et al., (1966), Parsegian and Gingell (1972), Ohshima et al., (1982), and Chan et al., (1995), and for unequal charges by Gregory (1975), and Ohshima (1995). The "Hogg-Healy-Fuerstenau" equation (Hogg et al., 1966) for two planar surfaces of low constant potentials in 1:1 electrolyte is

$$W(D) = \frac{\varepsilon_0 \varepsilon \kappa [2\psi_1 \psi_2 - (\psi_1^2 + \psi_2^2) e^{-\kappa D}]}{(e^{+\kappa D} - e^{-\kappa D})} \text{ J m}^{-2}$$
(14.61)

which leads to a pressure of

$$P(D) = -\frac{\mathrm{d}W}{\mathrm{d}D} = \frac{2\varepsilon_0 \varepsilon \kappa^2 [(e^{+\kappa D} + e^{-\kappa D})\psi_1 \psi_2 - (\psi_1^2 + \psi_2^2)]}{(e^{+\kappa D} - e^{-\kappa D})^2} \text{ N m}^{-2}.$$
 (14.62)

Approximate expressions for constant charge interactions are more complicated. The following, proposed by Gregory (1975), is probably the simplest that is also reasonably accurate for 1:1 electrolytes

$$P(D) = \rho_{\infty}kT \left[2\left\{ 1 + \left(\frac{ze(\psi_1 + \psi_2)/kT}{e^{+\kappa D/2} - e^{-\kappa D/2}} \right)^2 \right\}^{1/2} - \frac{\left\{ ze(\psi_1 - \psi_2)/kT \right\}^2 e^{-\kappa D}}{1 + \left(\frac{ze(\psi_1 + \psi_2)/kT}{e^{+\kappa D/2} - e^{-\kappa D/2}} \right)^2} - 2 \right] \text{ N m}^{-2}. \quad (14.63)$$

It is noteworthy that the double-layer forces between dissimilar surfaces can change sign, depending on the conditions. For example, for constant potential interactions at large separations, Eq. (14.62) tends to $P(\kappa D) = 2\varepsilon_0 \varepsilon \kappa^2 \psi_1 \psi_2 e^{-\kappa D}$. This is attractive when ψ_1 and ψ_2 have opposite signs and repulsive when they have the same sign, and it reduces

⁸For a colloidal system at equilibrium, all the interactions are given by the equilibrium interaction potentials even though the particles may be moving very rapidly in the solution. This is an example of *Detailed Balance*.

to Eq. (14.55) when $\psi_1=\psi_2$. However, in the limit of $D\to 0$, Eq. (14.62) tends to $P(D\to 0)=-\varepsilon_0\varepsilon\kappa\,(\psi_1-\psi_2)^2/2D^2$ which is always negative—that is, attractive.

The constant charge interaction at large separations, Eq. (14.63), reduces to $P(\kappa D) = 4(\rho_{\infty}z^2e^2/kT) \psi_1\psi_2e^{-\kappa D} = 2\varepsilon_0\varepsilon\kappa^2\psi_1\psi_2e^{-\kappa D} = 2\kappa^2\sigma_1\sigma_2e^{-\kappa D}/\varepsilon_0\varepsilon$, which is the same as the constant potential limit. However, in the limit of $D \to 0$, Eq. (14.63) tends to $P(D \to 0) = +|(\sigma_1 + \sigma_2) kT/zeD|$, which reduces to Eq. (14.59) when $\sigma_1 = \sigma_2$ and that is always positive—that is, repulsive (see Problem 14.4).

All of the above equations assume no charge regulation and that the surface charges are smeared out on each surface. Both of these assumptions are particularly dangerous when the two surfaces are different. Such surfaces usually contain ion-exchangeable sites, and their charges can often move about and redistribute as the surfaces come into contact. Some of these issues, especially those involving "competitive adsorption," have been addressed by Ninham and Parsegian (1971), Prieve and Ruckenstein (1976), Chan et al., (1980), Pashley (1981), Van Riemsdijk et al., (1986), Carnie and Chan (1993), and Ettelaine and Buscall (1995), and are discussed again in later sections devoted to acidbase interactions and the adhesion of amphoteric and biological surfaces.

At very large separations, above 1 µm or the dimensions of colloidal particles, there is experimental evidence that the double-layer force can become weakly attractive even between identical particles, which can result in phase separation (Ise and Yoshida, 1996). Sogami and Ise (1984) have proposed a potential—the "Sogami potential"—to account for this effect, but it remains controversial both at the experimental and theoretical levels.

Ion-Condensation and Ion-Correlation Forces 14.19

We may recall that for a system of charges that is overall electrically neutral the net electrostatic (purely Coulombic) interaction is always attractive. This is the attraction that leads to the formation of ionic crystals discussed in Section 3.4. However, as discussed further in Section 3.8, in a medium of high dielectric constant such as water, the Coulomb interaction is much reduced and thermal effects can now win out, causing the dissolution of the ionic crystal. An important parameter that always arises when considering such effects is the Bjerrum length $\lambda_{\rm B}$, which is the distance r between the centers of two unit charges when their Coulomb energy, $w(r) = e^2/4\pi\varepsilon_0\varepsilon r$, equals the thermal energy kT that is,

$$\lambda_{B} \,=\, e^{2}/4\pi\epsilon_{0}\epsilon kT \label{eq:lambda}$$

$$=\, 0.72\,\text{nm in water at }25^{\circ}\text{C}\,(\epsilon\,=\,78.3).$$

The Bjerrum length appears often in equations associated with electrostatic interactions in electrolyte solutions, such as double-layer, ion-condensation, and ion-correlation interactions. For example, the Debye length, Eq. (14.36), can be expressed as $\Sigma (4\pi\lambda_{\rm B}\rho_{\infty i}z_i^2)^{1/2}$, and the solubility of a 1:1 electrolyte, Eq. (3.18), can be expressed as $X_s \approx e^{-\lambda_B/(a_+ + a_-)}$, where $(a_+ + a_-)$ is the distance between the centers of the ions. In Section 3.8 we saw how this equation accounts for the higher solubility or dissociation of larger ions (larger $a_+ + a_-$). For example, when $(a_+ + a_-) = \lambda_B$ we expect full dissociation up to electrolyte concentrations of ~40% (mole/mole). For smaller and especially multivalent ions such as Ca²⁺, their tendency to dissociate is much reduced, and such electrolytes or salts are much less soluble, and their ions in solution are often only partially dissociated (or partially associated).

A similar effect arises at charged surfaces. Consider a small sphere of radius R where the surface charges are separated by a mean distance d such that the total charge on the sphere is $Q = (4\pi R^2/d^2)e$. The Coulomb energy of bringing a small ion of radius a and charge ze up to the sphere is $zeQ/4\pi\varepsilon_0\varepsilon(R+a)$. For small similarly sized monovalent ions (Q=e,z=1) this reduces to the expected equation: $w(r)=e^2/4\pi\varepsilon_0\varepsilon(2a)$, but for a large spheres $(R \gg a)$ we obtain for the ion-surface binding energy:

$$w \approx zeO/4\pi\varepsilon_0\varepsilon R \approx 4\pi zkTR\lambda_B/d^2$$
. (14.65)

This equation shows that at constant surface charge density (fixed d), the binding energy of a (counter)ion to an oppositely charged surface is higher (1) for larger spheres or particles (larger R), (2) the closer the surface co-ions are to each higher (smaller d, higher σ), and (3) the higher the valency, z, of the binding counterion. The first two conclusions show that the size of a macromolecule or small colloidal particle is important in determining its surface charge density σ and potential ψ_0 —the smaller the particle, the more likely it is to be fully ionized.

The strength of ion binding also depends on the shapes or geometry of particles, being stronger for planar surfaces, then cylindrical surfaces then spherical surfaces—an effect that is referred to as charge, ion or "Manning" condensation (Manning, 1969; Ray and Manning, 1996). For example, planar surfaces are generally less than 10% ionized or dissociated, cylindrical (DNA or micelle) surfaces are typically ~20% ionized, small spherical micelles are ~25% ionized (Pashley & Ninham, 1987), while individual ionizable molecules, which can be considered as very small spheres, are often fully (close to 100%) ionized. Equation (14.65) also shows why this effect is more pronounced for multivalent counterions.

The effect of ion condensation is a reduced double-layer repulsion, especially between planar and cylindrical structures such as clay sheets, charged lipid bilayers, DNA, nanorods and microtubules in aqueous solutions, which is further enhanced when these contain calcium or polyvalent ions (Bloomfield, 1991; Podgornik et al., 1994; Tang et al., 1996). In reality, the binding energy of ions to surfaces in electrolyte solutions is much more complex than given by Eq. (14.65) and depends, among other things, on the absolute or relative values of R, a, λ_B , d, and κ^{-1} .

Whereas ion-condensation simply lowers the double-layer repulsion, there is another counterion effect between similarly charged surfaces that gives rise to an attraction. This is contrary to the Poisson-Boltzmann equation that predicts a repulsion at all separations between equally charged surfaces. This additional electrostatic force was first proposed

by Oosawa (1971) who considered the implications of having mobile (rather than fixed) counterions in each double layer. These mobile ions, he argued, constitute a highly polarizable (essentially conducting) layer at each interface whose fluctuations in density must give rise to an attractive van der Waals-like force with another double-layer. This force is not included in the Poisson-Boltzmann equation nor in the Lifshitz theory. Now known as the ion-correlation or charge fluctuation force (Jonsson, 1980; Guldbrand et al., 1984: Kiellander, 1988a) this attraction becomes significant at small distances (<4 nm), and it increases with the surface charge density and valency of the counterions—just as does the ion-condensation effect with which it is often associated (Rouzina and Bloomfield, 1996; Gronbech-Jensen, 1997).

In the first Monte Carlo study of the ionic density distributions, interaction energies and pressures between planar surfaces, spheres and cylinders, Wennerström and colleagues (1982) concluded that between surfaces of high charge density the attractive ion-correlation force can reduce the effective double-layer repulsion by 10-15% if the counterions are monovalent. However, with divalent counterions such as Ca2+ the ioncorrelation attraction was found to exceed the double-layer repulsion—the net force becoming overall attractive—below about 2 nm, even in dilute electrolyte solutions. Such short-range attractive ion-correlation forces have been measured between anionic surfactant and lipid bilayers in CaCl₂ solutions, and they are believed to be responsible for the strong adhesion or limited swelling of negatively charged clay surfaces in the presence of divalent ions (Marra, 1986b, c; Khan et al., 1985; Kjellander et al., 1988a, b; Kjellander, 1990). Their importance in the interactions of colloidal, amphiphilic and biological surfaces have yet to be fully established.

Similar ion-correlation interactions can arise between the surface co-ions of two opposing surfaces if these are mobile, as occurs at surfactant and lipid bilayer and biological membrane surfaces. Indeed, it has been suggested that when both the counterions and coions are mobile, the final adhesion of the two surfaces can cause them to order into a thin crystalline lattice (Rouzina and Bloomfield, 1996). Such effects are usually specific and can be understood only by considering the surface charges as discrete and of a certain size rather than as smeared out over the surfaces (cf. Chapter 21).

Both ion-correlation and ion-condensation forces enhance adhesion; they are related (Rouzina, 1996; Shklovskii, 1999) but are difficult to separate, quantify or simulate and, so far, do not appear to be describable by a single simple force-law or potential function although some have been proposed (Lau et al., 2000). Experimental examples of both of these interactions are given in Part III.

Another effect that derives from the discreteness of surface charges is the "image force" produced by a surface coion and its image on the opposite surface. As shown in Figure 13.2, this produces a repulsive force when the two surfaces are in a medium (e.g., water) with a dielectric constant that is higher than those of the surfaces. However, Ohshima (1995) has argued that for certain charge-regulating mechanisms the image force can reduce the double-layer repulsion.

More Complex Systems: Finite Reservoir Systems 14.20 and Finite Ion-Size Effects

We have seen how different are the interactions between charged surfaces in the absence and presence of a bulk "infinite" reservoir of electrolyte ions at some given concentration. In many cases the situation is not so simple. For example, the case of "counterions only," discussed in Sections 14.2-14.9 changes when some electrolyte is present, and when the number of counterions coming off from the surfaces are comparable to the number of background electrolyte ions already present in the system, the equations for the ionic distributions and interaction forces become more complicated and can only be solved numerically (Dubois et al., 1992). Such systems arise when concentrated dispersions of clay sheets, micelles, bilayers or polyelectrolytes interact in pure water or dilute salt solutions (Dubois et al., 1992; Diederichs et al., 1985; Delville et al., 1993).

In some cases, simplifying assumptions can be made. Thus, it has been found that the Debye length of a micellar or polyelectrolyte solution is given by Eq. (14.36) but where only the background electrolyte ions and micellar or polyelectrolyte counterions contribute to the ionic concentrations in that equation but not the micelles or polyelectrolyte molecules themselves. For example, for a micellar system above the critical micelle concentration (cmc) consisting of completely dissociated surfactant monomers at a concentration $X_{\rm cmc}$ coexisting with micelles of concentration $X_{\rm mic}$ and aggregation number N of which a fraction f are ionized (typically $f \approx 0.25$), the Debye length is given by (Pashley and Ninham, 1987)

$$\kappa^2 = \frac{e^2}{\varepsilon_0 \varepsilon kT} [2X_{\rm cmc} + (NX_{\rm mic} - X_{\rm cmc})f]. \tag{14.66}$$

Tadmor and colleagues (2002) derived a similar equation for polyelectrolyte solutions.

Finite ion size effects can play an important role in modifying the double-layer interactions between surfaces at small separations. First, as discussed in Section 14.6, the existence of a Stern Layer due to finite coion and/or counterion sizes does not necessarily affect the functional form of the ionic distribution away from a surface; but it does shift the plane of origin of the distribution (the Outer Helmholtz Plane or OHP) which effectively changes the way D=0 is defined in equations for the forces. As will be discussed further below, this can have important consequences in the presence of another force, such as the van der Waals force, which may have a different plane of origin. Similar finite size effects arise in the case of van der Waals forces, but now with respect to the solvent molecules, as described in Chapter 15.

The previous sections have revealed the great complexity of double-layer forces, almost to the point where it may appear than any interaction is possible. However, as we shall see, there are many situations where the measured forces appear to be well described by the simplest continuum equations, such as those in Figure 14.10, right down to molecular contact.

14.21 Van der Waals and Double-Layer Forces Acting Together: the DLVO Theory

The total interaction between any two surfaces must also include the van der Waals attraction. Now, unlike the double-layer interaction, the van der Waals interaction potential is largely insensitive to variations in electrolyte concentration and pH, and so may be considered as fixed in a first approximation. Further, the van der Waals attraction must always exceed the double-layer repulsion at small enough distances since it is a power law interaction (i.e., $W \propto -1/D^n$), whereas the double-layer interaction energy remains finite or rises much more slowly as $D \to 0$. Figure 14.13 shows schematically the various types of interaction potentials that can occur between two similarly charged surfaces or colloidal particles in a 1:1 electrolyte solution under the combined action of these two forces. Depending on the electrolyte concentration and surface charge density or potential one of the following may occur:

- For highly charged surfaces in dilute electrolyte (i.e., long Debye length), there is a strong long-range repulsion that peaks at some distance, usually between 1 and 5 nm, at the *force* or *energy barrier*, which is often high (many kT).
- In more concentrated electrolyte solutions there is a significant secondary minimum, usually beyond 3 nm, before the energy barrier closer in. The potential energy minimum at contact is known as the *primary minimum*. For a colloidal system, even though the thermodynamically equilibrium state may be with the particles in contact in the deep primary minimum, the energy barrier may be too high for the particles to

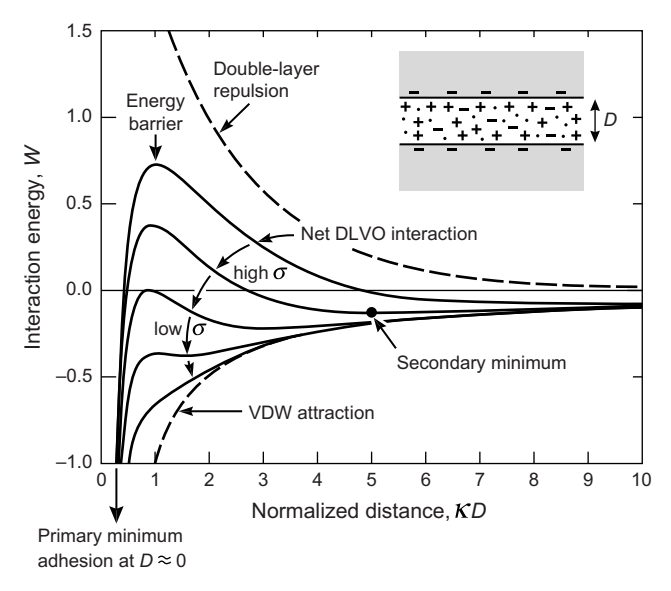


FIGURE 14.13 Schematic energy versus distance profiles of the DLVO interaction. The actual magnitude of the energy W is proportional to the particle size (radius) or interaction area (between two planar surfaces).

overcome during any reasonable time period. When this is the case, the particles will either sit in the weaker secondary minimum or remain totally dispersed in the solution. In the latter case the colloid is referred to as being kinetically stable (as opposed to thermodynamically stable).

- For surfaces of low charge density or potential, the energy barrier will be lower. This leads to slow aggregation, known as coagulation or flocculation. Below a certain charge or potential, or above some concentration of electrolyte, known as the critical coagulation concentration, the energy barrier falls below the W=0 axis (middle curve in Figure 14.13) and the particles then coagulate rapidly. The colloid is now referred to as being unstable.
- As the surface charge or potential approaches zero the interaction curve approaches the pure van der Waals curve (lower dashed curve in Figure 14.13), and two surfaces now attract each other strongly at all separations.

The sequence of phenomena described above can be described quantitatively (see Worked Examples 14.5 and 14.6), and it forms the basis of the celebrated DLVO theory of colloidal stability, after Derjaguin and Landau (1941), and Verwey and Overbeek (1948). See also Hiemenz (1997), Hunter (2001), and Evans and Wennerström (1999).

The main factor inducing two (negatively charged) surfaces to come into adhesive contact in a primary minimum is the lowering of their surface charge or potential, brought about by decreasing the pH, increased cation binding, or increasing the screening of the double-layer repulsion by increasing the salt concentration. If the double-layer repulsion remains high on raising the salt concentration, two surfaces can still "adhere" to each other, but in the secondary minimum, where the adhesion is much weaker and easily reversible. On the other hand, as discussed below, in Section 14.16 and in Chapter 15, there are situations where particles first aggregate then redisperse as the salt concentration or pH is increased.

It is clear that one must have a fairly good idea of the charging process occurring at a surface before attempting to understand its double-layer interactions and the stability of colloidal dispersions, as Worked Examples 14.5 and 14.6 show.

Worked Example 14.5

Question: For a biocolloidal dispersion of 0.1 µm radius vesicles in a 100 mM NaCl solution at 37°C it has been established that the surface potential ψ_0 changes linearly with increasing pH from $\psi_0 = +50$ mV at pH 5 to $\psi_0 = -50$ mV at pH 7. Assuming that the vesicle dispersion remains effectively stable for energy barriers greater than about 25 kT, calculate the range of pH over which the system is unstable—that is, the vesicles aggregate. Assume a Hamaker constant for the vesicles in the solution of $A = 10^{-20}$ J.

Answer: The vesicle-vesicle interaction energy at 37°C is $W(D) = \frac{1}{2}RZe^{-\kappa D} - AR/12D = (0.5 \times 10^{-7}) \times (9.38 \times 10^{-11}) \tanh^2(\psi_0/107)e^{-\kappa D} - (10^{-20} \times 10^{-7})/12D = (4.69 \times 10^{-18}) \tanh^2(\psi_0/107) e^{-D(\text{nm})/0.95} - (8.33 \times 10^{-20})/12D(\text{nm})$. Figure 14.14 shows the DLVO plots at $\psi_0 = \pm 24.5$ mV (the "critical coagulation potential" where the energy

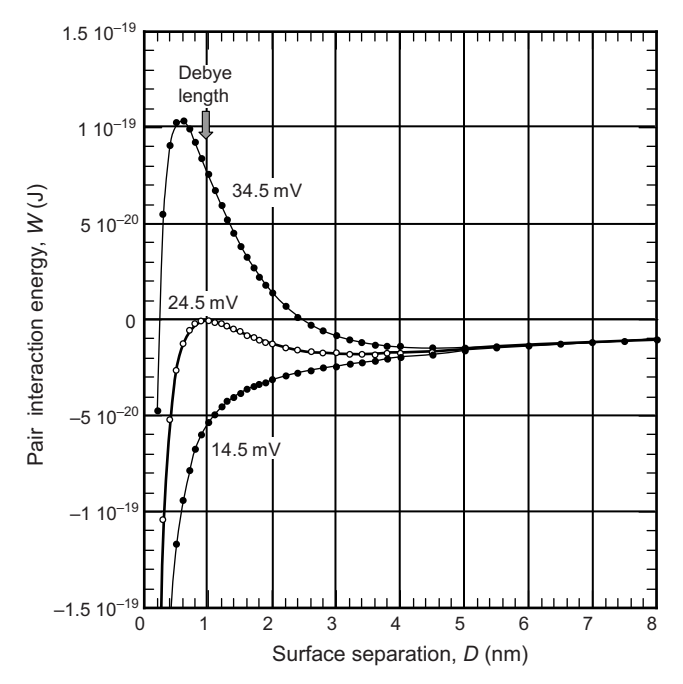


FIGURE 14.14 Computed DLVO energy profiles between amphoteric vesicles of radii 1,000 Å (0.1 μ m) in 100 mM NaCl solution at 37°C. Note that at the "critical coagulation potential" (middle curve) the energy maximum at W=0 occurs at the Debye length ($D=\kappa^{-1}=0.95$ nm in 100 mM NaCl).

is everywhere negative resulting in rapid coagulation) as well as at ± 14.5 and ± 34.5 mV—that is, 10 mV on either side of the critical potential. The energy barrier exceeds $25~kT=1.1\times 10^{-19}$ J for potentials higher than about 35 mV (positive or negative), which correspond to pH values of 35/50=0.7 above or below pH 6.0 (the "isoelectric point" or pI where $\psi_0=0$). Thus, the vesicles will aggregate at pH values between 5.3 and 6.7, although rapid coagulation will occur at pH values between 5.5 and 6.5. Strictly, the answer also depends on the vesicle concentration and on the depth of the primary minimum. The secondary minimum at ~4.5 nm is of depth 1.5×10^{-20} J or 3.5~kT, which is not deep enough to cause aggregation except for larger vesicles at higher vesicle concentrations.

Worked Example 14.6

Question: For a number of colloidal systems it is found that the "critical coagulation concentration" (ccc) of the *electrolyte* varies with the inverse sixth power of the counterion valency z—that is, $\rho_{\infty}(\text{ccc}) \propto 1/z^6$. Is this empirical observation, known as the Schultze-Hardy rule, (Schultze, 1882, 1883; Hardy, 1900), consistent with the DLVO theory?

Answer: The total DLVO interaction potential between two spherical particles interacting at constant potential is

$$W(D) = (64\pi k T R \rho_{\infty} \gamma^{2} / \kappa^{2}) e^{-\kappa D} - AR/12D$$
 (14.67)

By definition (see Figures 14.13 and 14.14), the critical coagulation concentration or condition occurs when both W = 0, and dW/dD = 0. The first condition leads to

$$k^2/\rho_{\infty} = 768\pi kTD\gamma^2 e^{-\kappa D}/A$$

while the second condition leads to $\kappa D = 1$, which shows that the potential maximum occurs at $D = \kappa^{-1}$ (the Debye length) as illustrated in Figure 14.14. Inserting this into the above equation leads to

$$\kappa^3/\rho_{\infty} = 768\pi k T \gamma^2 e^{-1}/A,$$

that is,

$$\kappa^6/\rho_\infty^2 \propto (T\gamma^2/A)^2$$
.

Now, since $\kappa^2 \propto \rho_{\infty} z^2/\varepsilon T$, the above equation implies that

$$z^6 \rho_{\infty} \propto \varepsilon^3 T^5 \gamma^4 / A^2, \tag{14.68}$$

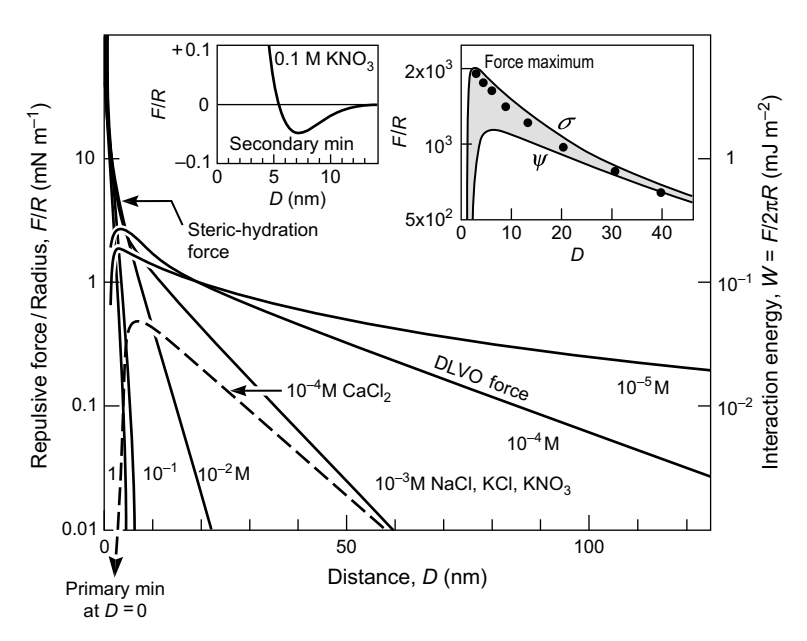


FIGURE 14.15 DLVO forces measured between two negatively charged mica surfaces in monovalent (10⁻⁵ to 1 M NaCl, KCl, KNO₃) and divalent (10⁻⁴ M CaCl₂) solutions. The shaded band in the right inset is the theoretical DLVO force in 10^{-4} M 1:1 electrolyte using a Hamaker constant of $A = 2.2 \times 10^{-20}$ J showing the constant charge σ and constant potential ψ limits. Theoretically, within the Poisson-Boltzmann formalism, we expect the interaction to fall between these two limits. At low ionic strengths, the forces are in good agreement with the DLVO theory right down to adhesive molecular contact in the primary minimum at D=0. The left inset is the measured force in concentrated 0.1-1.0 M KNO₃ showing the emergence of a secondary minimum, and at even smaller separations there is an additional repulsive short-range steric-hydration force believed to be due to the finite hydrated size of the adsorbed monovalent cations (see Figure 14.7). Figure 14.18 shows a similar effect. [Data from SFA experiments with surfaces in the crossed-cylinder geometry, equivalent to a sphere of radius R near a flat surface or two spheres of radius 2R, from Israelachvili and Adams, 1978; Pashley, 1981a; and Israelachvili, 1982.]

which is a constant if γ is constant, a condition that holds at high surface potentials ($\psi_0 > 100$ mV) where $\gamma = \tanh(ze\psi_0/4kT) = 1$. In this limit, therefore, the critical coagulation concentrations do indeed scale as $\rho_{\infty} \propto 1/z^6$. For example, if coagulation occurs at 1 M with a 1:1 electrolyte, it will occur at $\frac{1}{64}$ M with a 2:2 electrolyte (or divalent counterions), and at $\frac{1}{729}$ M with a 3:3 electrolyte (or trivalent counterions). Thus, the Schultze-Hardy rule is consistent with the DLVO theory.

But wait. Is it not unreasonable to assume high surface potentials in divalent and trivalent electrolyte solutions? Let us investigate the case of low potentials. Here we have $\gamma \propto z \psi_0 / T$, so that Eq. (14.68) now becomes

$$z^2 \rho_{\infty} \propto \varepsilon^3 T \psi_0^4 / A^2, \tag{14.69}$$

which is constant if ψ_0 remains constant. Thus for low but constant potentials we obtain a modified form of the Schultze-Hardy rule: $\rho_{\infty} \propto 1/z^2$.

In real systems the surface potential is neither high nor constant, but usually falls to quite low values as the valency of the electrolyte counterions increases. For example, if $\psi_0 \propto 1/z$, then for low potentials we now obtain: $\rho_{\infty} \propto \psi_0^4/z^2 \propto 1/z^6$, which brings us back to the Schultze-Hardy rule. Clearly, the DLVO theory can be applied in more ways than one to explain the Schultze-Hardy rule.

Probably the most important practical issue in any quantitative interpretation of experimental results in terms of the DLVO theory is the question of the locations of the "planes of origin" of the double-layer and van der Waals forces. For the double-layer interaction D = 0 is defined at the plane where the PB equation commences to be valid that is, at the OHP, which is generally at or a few angstroms farther out from the physical substrate-liquid interface due to the finite size of the surface coions or adsorbed counterions (14.4, 14.7 and 14.18) or the protruding or mobile surface-attached co-ions (Figures 15.14, 16.14, and Chapter 21). On the other hand, for the van der Waals force D =0 is defined as the distance between the atomic or ionic centers, which is ~2Å farther in from the physical solid-liquid interface (cf. Section 13.13). A difference of δ in the locations of D=0 per surface (2 δ for both surfaces) pushes the plane of origin of the doublelayer interaction (the OHP) out to $D=2\delta$ relative to the van der Waals interaction, which can totally change the DLVO interaction potential. It is remarkable that for values of δ as small as 0.2-0.3 nm the energy barrier and deep primary minimum can be totally eliminated, the force-law becomes repulsive at all separations down to "steric contact" at D = 2δ , and its profile can be significantly modified out to distances as far as 5 nm (see Figs 15.14 and 15.15). This model was first proposed by Frens and Overbeek (1972) to explain the common phenomenon of colloidal stability in high salt, the spontaneous swelling of certain colloids in water, and repeptization—the reversible coagulation of colloidal particles (according to the DLVO theory coagulation in a primary minimum should never be reversible). This effect was later demonstrated experimentally by Marra and Israelachvili (1985) for charged lipid bilayers, by Vigil et al., (1994) for silica surfaces, and by Claesson et al., (1984) for adsorbing *counterions* (see Figure 14.18).

Worked Example 14.7

Question: The osmotic limit of Eq. (14.59) assumes that the trapped counterions have zero size. Applying the same finite-size correction as in the van der Waals equation of state, show that this introduces an effective Stern Layer of thickness $\delta = 16\pi a^3 \sigma/3e$ per surface, where a is the ionic radius and σ the surface charge density. What is δ for (i) unhydrated and (ii) hydrated sodium counterions when each surface charge occupies an area of 1 nm²?

Answer: The van der Waals excluded volume correction to the pressure is P = kT/(V-b), where we may write V = AD for surfaces of area A interacting across a gap width D. Thus, P = kT/(AD - b) = kT/A(D - b/A), which effectively shifts the force curve for point counterions F = PA = kT/D outwards by D = b/A. Since $b = 4 \times$ total ionic volume in the gap = $4(2\sigma A/e)\frac{4}{3}\pi a^3$, the magnitude of this shift is

$$\delta = b/2A = 16\pi a^3 \sigma/3e$$
 per surface,

where σ/e is the number of charged sites per unit area. Thus, the *free* counterions in the diffuse double-layer increase the range of the short-range double-layer repulsion in the same way as does a finite Outer Helmholtz Plane or Stern Layer of thickness δ , which are normally associated with the surface co-ions or surface-bound counterions. Further aspects of this effect are discussed by Marcelja (1997, 2000). For a charge density of 1 nm² per unit charge $(\sigma/e = 10^{18} \text{ m}^{-2})$, inserting a = 0.095 nm for the radius of unhydrated sodium ions (Table 4.2) gives $\delta = 0.014$ nm. In contrast, for hydrated ions, where $a \approx 0.36$ nm, we obtain $\delta \approx 0.8$ nm, which is a 50-fold increase that can have a very dramatic effect on the net DLVO interaction (see Worked Example 15.3).

14.22 Experimental Measurements of Double-Layer and DLVO Forces

Figure 14.15 shows the experimental results of direct force measurements between two mica surfaces in dilute 1:1 and 2:1 electrolyte solutions where the Debye length is large, thereby allowing accurate comparison with theory to be made at distances much smaller than the Debye length. The theoretical DLVO force laws (using exact solutions to the nonlinear PB equation, which differ from the approximate equations of Section 14.16 only below κ^{-1}) are shown by the continuous curves. The agreement is remarkably good at all separations, even down to 2% of κ^{-1} , and indicates that the DLVO theory is basically sound. One may also conclude that the dielectric constant of water must be the same as the bulk value even at surface separations as small as 2 nm, since otherwise significant deviations from theory would have occurred (Hamnerius et al., 1978, showed that the dielectric constant of water remains unchanged even in 1 nm films). The surface potentials ψ_0 inferred from the magnitude of the double-layer forces agree within 10 mV with those measured independently on isolated mica surfaces by the method of electrophoresis (Lyons et al., 1981). Further, the surface charge density corresponding to

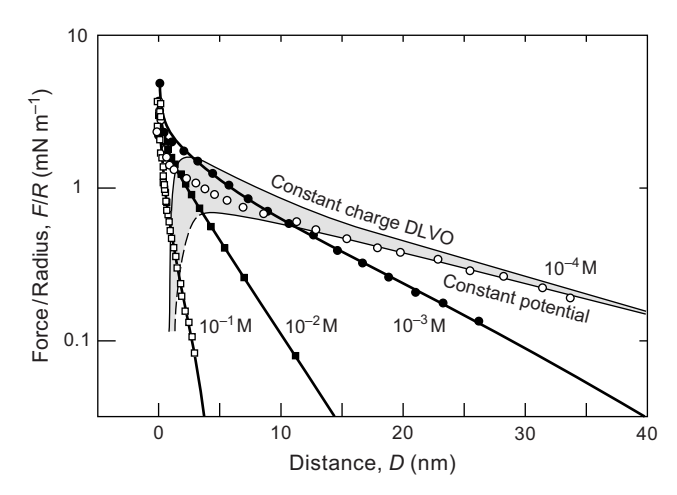


FIGURE 14.16 The first accurate measurement of double-layer forces using AFM, between a silica bead of radius R ~ 1.5 μm and a flat silica surface in aqueous NaCl solutions. Note how the repulsive short-range double-layer and "hydration" forces increase with increasing ionic strength even though the range of the long-range double-layer repulsion decreases —an effect also seen in the forces between other surfaces such as mica (Figure 14.15). [Reproduced from Ducker and Senden, 1992, with permission, I

these potentials is typically 1e per 60 nm². Thus, at separations below about 8 nm the surfaces are actually closer to each other than the mean distance between the surface charges, and yet the double-layer forces still behave as if the surface charges are smeared out. The reason for this will become clear in section 14.24.

Figure 14.16 shows the first AFM measurement of double-layer forces between two silica surfaces, by Ducker et al., (1991). Again the results are in good agreement with theory except at small separations where no adhesion was measured. As mentioned in the previous section, in the case of silica the lack of adhesion in aqueous electrolyte solutions is believed to be due to the protruding silicic acid groups on the silica surface, which carry the negative charges and define the OHP (see also Section 15.8 and Vigil et al., 1994).

Other SFA, AFM and Osmotic Pressure measurements of double-layer or DLVO forces have been carried out in various monovalent, divalent and multivalent electrolyte solutions (Pashley, 1981a,b, 1984; Pashley and Israelachvili, 1984; Horn et al., 1988a), between surfactant and lipid bilayers (Pashley and Israelachvili, 1981; Marra, 1986b,c; Marra and Israelachvili, 1985; Claesson and Kurihara, 1989; Pashley et al., 1986; Diederichs et al., 1985; Dubois et al., 1992; Delville et al., 1992, 1993; Anderson et al., 2010), across soap films (Derjaguin and Titijevskaia, 1954; Lyklema and Mysels, 1965; Donners et al., 1977), between silica, sapphire, and metal or metal oxide surfaces (Horn et al., 1988a, 1989; Smith et al., 1988; Meagher, 1992; Vigil et al., 1994; Larson et al., 1993), as well as in nonaqueous polar liquids (Christenson and Horn, 1983, 1985). The results on surfactant and lipid bilayers, and on biological molecules and surfaces, are discussed in more detail in later sections devoted to amphiphilic and biological systems. Here we shall concentrate more on solid, inorganic surfaces.

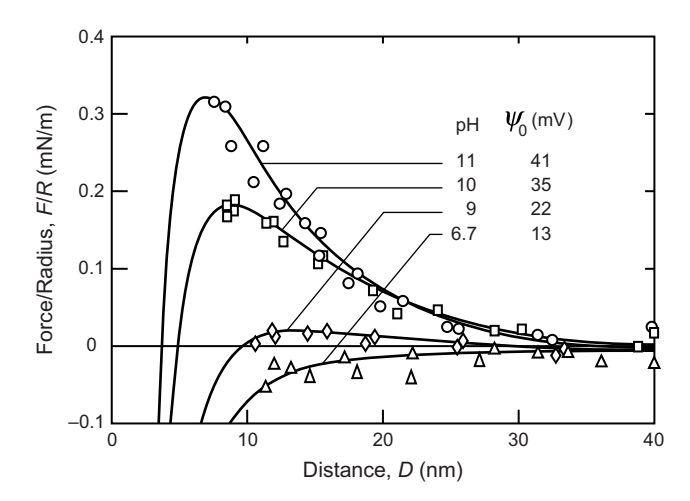


FIGURE 14.17 Classic DLVO forces measured between two sapphire surfaces in 10⁻³ M NaCl solutions at different pH. The continuous lines are the theoretical DLVO forces for the potentials shown and a Hamaker constant of $A = 6.7 \times 10^{-20}$ J. [Data from SFA experiments with surfaces in the crossed-cylinder geometry, equivalent to a sphere of radius R near a flat surface or two spheres of radius 2R, adapted from Horn et al., 1988a.]

In general, the results have been in good agreement with the DLVO theory (Figure 14.17), often down to separations well below the Debye length (see Figure 14.15). When deviations do occur these can usually be attributed to the presence of other, non-DLVO, forces or to the existence of a Stern-layer or protruding coions. A direct experimental measurement of Stern-layer stabilization is shown in Figure 14.18 where the counterions used in that study where unusually large. This shows that a short-range stabilizing repulsion, even in high salt, does not necessarily imply the existence of an additional non-DLVO force (such as a solvation or hydration force, discussed in Chapter 15). But it does require an explanation for what determines the finite value for δ .

As already noted, for certain geometries the double-layer repulsion at constant potential decreases at long-range but increases at short range with increasing ionic strength. This effect may explain the coagulation of colloidal particles and the collapse of certain charged polymers with increasing salt, followed by their redispersal and reexpansion on further increasing the concentration (Kallay et al., 1986; Drifford et al., 1996).

It is perhaps surprising that measured double-layer forces are so well described by a theory that, unlike van der Waals force theory, contains a number of fairly drastic assumptions, viz. the assumed smearing out of discrete surface charges, that ions can be considered as point charges, the ignoring of image forces, and that the PB equation remains valid even at small distances and high concentrations. One reason for this is that many of these effects act in opposite directions and tend to cancel each other out. As mentioned above, most experimental deviations in the forces from those expected from the DLVO theory are not due to any breakdown in the DLVO theory, but rather to the existence of a Stern-layer or to the presence of other forces such a ion-correlation,

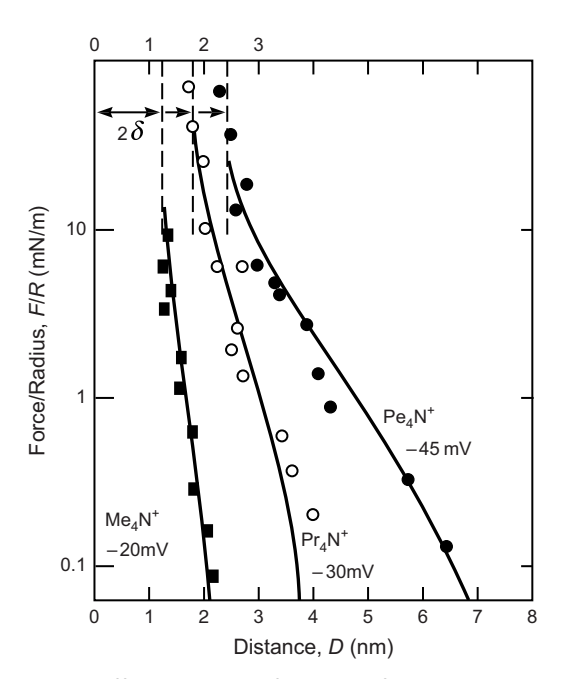


FIGURE 14.18 Example of Stern-layer effects due to the finite size of the counterions. Measured forces between two mica surfaces in various tetra-alkyl ammonium bromide solutions (Claesson et al., 1984). The continuous curves are the expected DLVO interactions assuming potentials as shown and Stern-layer thicknesses of δ per surface egual to the diameters (Born repulsion) of the adsorbed cations: $\delta = 0.6$ nm for methyl ammonium (Me₄N⁺), $\delta = 0.9$ nm for propyl ammonium (Pr_4N^+), and $\delta = 1.2$ nm for pentyl ammonium (Pe_4N^+). Note how the outward shift in the OHP has eliminated the force maximum and primary minimum. [Data from SFA experiments with surfaces in the crossed-cylinder geometry, equivalent to a sphere of radius R near a flat surface or two spheres of radius 2R.]

solvation, hydrophobic, or steric forces. These additional forces, are, of course, very important, especially in more complex colloidal and biological systems where they often dominate the interactions at short-range where most of the interesting things happen. Their consideration forms a large part of the rest of this book.

14.23 **Electrokinetic Forces**

When an electric field is applied across an electrolyte solution, any charged particles suspended in the solution will move toward the oppositely charged electrode—for example, a negatively charged colloidal particle will move toward the anode. This is known as electrophoretic flow and the force acting on the particle is known as the electrophoretic force. With regard to the electrolyte ions themselves, these will also move, the anions toward the anode and the cations toward the cathode. If the surfaces of the flow chamber are charged—for example, if the field is applied along a silica capillary tube whose surface is negatively charged—then the excess positively charged counterions in the solution will move toward the cathode. Since these counterions will be located within the double-layer very close to the surface, the whole liquid column enveloped by these ions (including any particles within the column) will be dragged along with them. This is known as electro-osmotic flow.

The forces, flows and flow patterns generated by electrophoretic and electro-osmotic forces can be extremely complex, and depend on the geometry and size of the flow chamber and the suspended particles. For example, the negatively charged particle moving toward the anode by electrophoresis will also experience an opposing electroosmotic force arising from the viscous drag of the suspending liquid moving in the opposite direction. If the diameter of the capillary tube is large compared to the diameter of the particle, the electrophoretic force wins out, but if it is small, the electro-osmotic force wins out and the particle will move with the liquid (Sen Gupta and Papadopoulos, 1997; Papadopoulos, 1999).

14.24 **Discrete Surface Charges and Dipoles**

The charge on a solid surface is obviously not uniformly spread out over the surface, as has been implicit in all the equations derived so far. For a surface with a typical potential of 75 mV in a 1 mM NaCl solution, the surface charge density as given by the Grahame equation is $\sigma = 0.0075$ C m⁻², which corresponds to only one charge per 21 nm² or 2100 Å². In 0.1 M NaCl the same potential implies 1e per 2 nm². Thus, the charges on real surfaces are typically 1-5 nm apart from each other on average. What effect does this have on the electrostatic interaction between two surfaces, especially at surface separations closer than the separation between the charges?

Let us consider a planar square lattice of like charges q as shown in Figure 14.19a. If d is the distance between any two neighboring charges, then the mean surface charge density is $\sigma = q/d^2$, and if this charge were smeared out, the electric field emanating from the surface would be uniform and given by $E_z = \sigma/2\varepsilon\varepsilon_0$. What, then, is the field of a surface lattice of discrete charges having the same mean charge density? To compute this field one must sum the contributions from all the charges. The resulting slowly converging series can be turned into a rapidly converging series by using a mathematical technique known as the Poisson summation formula (Lighthill, 1970). If x and y are the coordinates in the plane relative to any charge as the origin (Figure 14.19a), the field E_z along the zdirection is given by the series (Lennard-Jones and Dent, 1928)

$$E_{\rm z} = \frac{\sigma}{2\varepsilon_0 \varepsilon} \left[1 + 2 \left(\cos \frac{2\pi x}{d} + \cos \frac{2\pi y}{d} \right) e^{-2\pi z/d} + \cdots \right],\tag{14.70}$$

where the higher-order terms decay much more rapidly with distance z. The first term is the same as that of a smeared-out surface charge. The second term is interesting, for it shows that the excess field decays away extremely rapidly, with a decay length of $d/2\pi$, for example, about 0.3 nm for charges 2 nm apart. Thus, at $z=\frac{1}{2}d$ the electric field is at most 17% different from that of the smeared-out field, while at z = d it has reached 99.3% of the smeared-out value! A similar conclusion is reached for other types

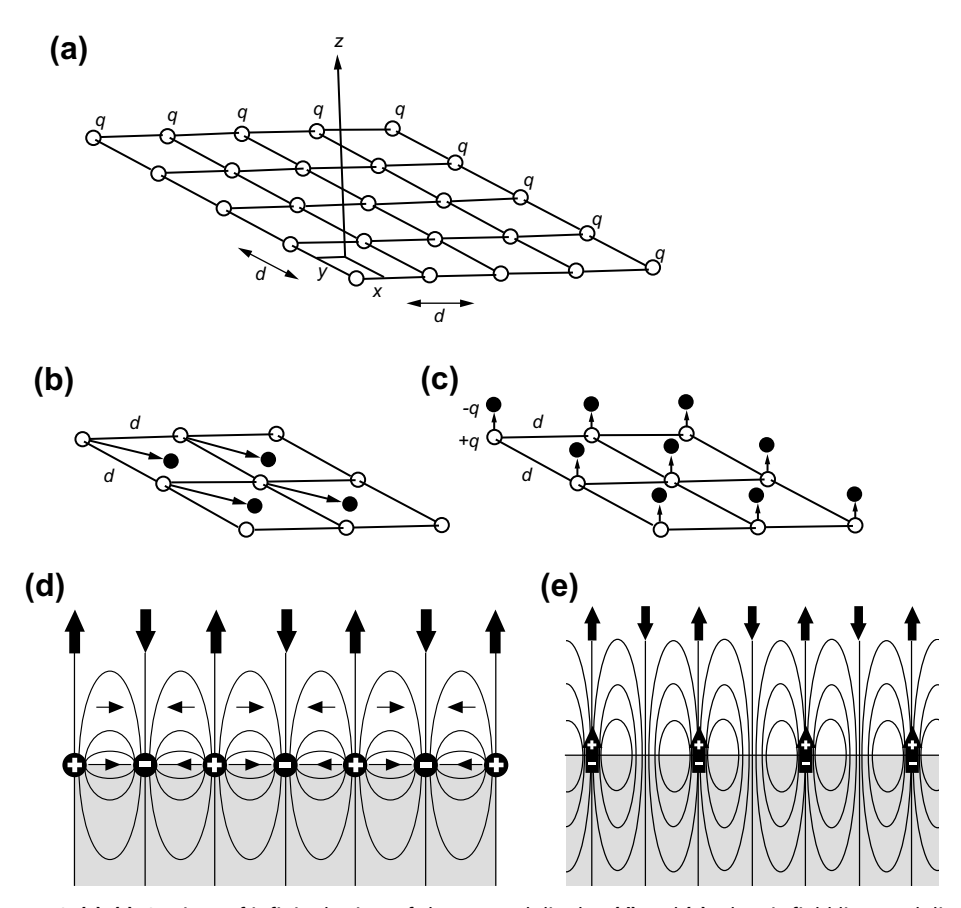


FIGURE 14.19 (a)–(c): Sections of infinite lattices of charges and dipoles. (d) and (e): Electric field lines and directions above electro-neutral surfaces consisting of discrete charges (d) and aligned dipoles (e). Equations (14.71) and (14.72) show that within a very short distance away from each surface ($z \ge d$) the average or mean field of a dipolar lattice is already effectively zero.

of lattices; for example, for a hexagonal lattice where neighboring ions are separated by a distance d, the mean surface charge density is $\sigma = 2q/\sqrt{3}d^2$ and the exponential decay length of the field is $\sqrt{3}d/4\pi$, which is even smaller than for a square lattice—that is, the field decays even faster. It is for these reasons that the smeared-out approximation works so well in considering the electrostatic interactions at and between charged surfaces (McLaughlin, 1989).

The above analysis can be readily extended to surfaces that have no net charge but that carry discrete surface dipoles. A common example of this is the dipolar or zwitterionic headgroups of lipid molecules that reside at the lipid-water interfaces of micelles, surface monolayers, and bilayers. The dipoles may align normally or parallel to the surfaces, and they can be either immobilized in a 2-D lattice or have (usually restricted) lateral and/or rotational mobility. The charged lattice of Figure 14.19a can be transformed into a lattice

of in-plane dipoles by adding charges of opposite sign at the center of each square (Figure 14.19b). By superimposing the fields of the positive and negative lattices using Eq. (14.70) it is easy to show that the electric field opposite a positive charge (at x = 0, v=0) is

$$E_{\rm z} = +(4q/\varepsilon_0 \varepsilon d^2) e^{-2\pi z/d} + \cdots, \tag{14.71}$$

while opposite a negative charge (at $x = \frac{1}{2}d$, $y = \frac{1}{2}d$), it is

$$E_z = -(4q/\varepsilon_0 \varepsilon d^2)e^{-2\pi z/d} + \cdots$$
 (14.72)

This geometry is equivalent to a dipolar or zwitterionic lattice whose dipoles, of length $d/\sqrt{2}$ and surface density $1/d^2$, are lying parallel to the surface.

For dipoles of length l comparable to d arrayed perpendicular to the surface, as in Figure 14.19c, the above two equations become replaced by $E_z \approx \pm (2q/\epsilon_0 \epsilon d^2) e^{-2\pi z/d} + \cdots$. This procedure can be readily extended to other lattices including three-dimensional ionic crystals. The end result is always that the field is positive or negative depending on the x, y coordinates and that it decays very rapidly to zero with increasing z.

If a second lattice of vertical dipoles is brought up to the first, the Coulombic interaction pressure between the two dipolar surfaces at a separation D will be given by

$$P(D) = \pm (2q^2/\epsilon_0 \epsilon d^4) e^{-2\pi D/d}$$
 (14.73)

depending on whether the approaching dipoles are exactly opposite each other or in register (+ sign, repulsion) or out of register (- sign, attraction). The pressure is anyway very small and in reality, since surface dipoles will not be on a perfect lattice but distributed randomly or moving about (e.g., zwitterionic head-groups on a lipid bilayer surface), the net pressure will average to zero in a first approximation, though a Boltzmannaveraged interaction will yield a weak but overall exponentially attractive force. A similar result is obtained if the dipoles are lying in the plane of the surfaces, as in Figure 14.19b.

The above results furnish yet another example of where the purely electrostatic interaction between a system of charges or dipoles that are overall electrically neutral produces an attractive force even though intuitively one might have expected two surfaces with vertical dipoles pointing towards each other to always repel each other. In the limit where the surface-bound dipoles are free to rotate in all directions the resulting interaction energy must be the same as the attractive van der Waals-Keesom interaction, which decays as $-1/D^4$ [Eq. (13.49)] but is screened if the interaction occurs across electrolyte solution (Section 13.11). Jönsson and Wennerström (1983) also considered the image force between individual dipoles and their image reflected by the other surface, and found that for surfaces of low dielectric constant interacting across water this contribution can be large and repulsive.

The interactions of finite-sized dipolar domains on surfaces, as occur in monolayers, lipid bilayers and biological membranes, are discussed in Chapters 20 and 21 (see also Problem 14.1).

PROBLEMS AND DISCUSSION TOPICS

- **14.1** Sketch the electric field lines of (i) a single dipole, (ii) an infinite lattice of vertical dipoles, and (iii) an infinite lattice of in-plane dipoles. Indicate the directions of the dipoles and fields with arrows. (iv) Without resorting to complex mathematical calculations show whether the normal Coulomb (dipole-dipole) force F(z) between two similar parallel surfaces of type (ii) and (iii) is attractive or repulsive. Assume that the *surfaces* (not the *fixed dipoles* on each surface) can move freely in the x-y plane. (v) Sketch the electric field lines of a *finite* lattice of dipoles of type (ii) and (iii).
- **14.2** A glass surface is exposed to water vapor at 96% relative humidity (i.e., $p/p_{\text{sat}} =$ 0.96). Estimate the equilibrium thickness D of the thin film of water adsorbed on the surface assuming (i) that only electrostatic double-layer forces are operating and that the surface is fully dissociated with a surface charge density of $\sigma =$ -0.1 C/m^2 , (ii) that the monovalent counterions (z=1) are uniformly distributed throughout the thin water film. [Answer: 0.46 nm.] With these same assumptions also estimate the repulsive electrostatic pressure between two such planar surfaces immersed in water at a distance 2D apart. [Answer: 5.6×10^6 Pa or 55 atm.] Is your estimate likely to be too high or too low, and how does it compare with the attractive van der Waals pressure between the surfaces at this separation? Will the van der Waals attraction eventually win out at some smaller, but physically realistic, plate separation? [Answer: ~0.4 nm.]
- **14.3** Calculate the repulsive pressure between two charged surfaces in pure water where the only ions in the gap are the counterions that have come off from the dissociating surface groups (i.e., no electrolyte present, no bulk reservoir). Assume a surface charge density of one electronic charge per 0.70 nm² and T = 22°C. Plot your results as pressure against surface separation in the range 0.5–18 nm and compare these with the experimental results of Cowley et al., [Biochemistry, Vol. 17, 3163 (1978)] where in Figure 4b on page 3166 the authors plot their measured values for such a system (\triangle points). What conclusions do you arrive at concerning the "hydration" forces between two pure phosphatidyl-glycerol (PG) bilayers at small separations?
- **14.4** Explain, in qualitative terms, why the double-layer interaction between two surfaces having unequal but constant charge densities is always repulsive at small separations, irrespective of the signs of σ_1 and σ_2 , and without resorting to complicated equations or mathematics show that it is given by $P(D \rightarrow 0) = +|(\sigma_1 + \sigma_2) kT/zeD|$, as given by Eq. (14.63) in this limit.
- **14.5** Split the double-layer interaction free energy into its enthalpic and entropic components and discuss the implications of your result.
- **14.6** The reason(s) why positively charged divalent counterions such as Ca²⁺ are better coagulants or flocculants of negatively charged surfaces or particles than monovalent ions such as Na⁺ is because of one or more of the following:
 - (i) They screen the electrostatic repulsion better.
 - (ii) They are more hydrated.